No strong CP violation up to the one-loop level in a two-Higgs-doublet model

P. M. Ferreira$^{(1,2)\ddagger}$ and L. Lavoura$^{(3)\S}$

$^{(1)}$ Instituto Superior de Engenharia de Lisboa — ISEL, 1959-007 Lisboa, Portugal

$^{(2)}$ Centro de Física Teórica e Computacional, Faculdade de Ciências, Universidade de Lisboa,
Av. Prof. Gama Pinto 2, 1649-003 Lisboa, Portugal

$^{(3)}$ Universidade de Lisboa, Instituto Superior Técnico, CFTP,
Av. Rovisco Pais 1, 1049-001 Lisboa, Portugal

June 12, 2019

Abstract

We put forward a two-Higgs-doublet model, furnished with a $\mathbb{Z}_3$ symmetry, wherein CP is conserved in the dimension-four terms of the Lagrangian and is softly broken in the scalar potential. The new particles of our model are one neutral scalar H, one neutral pseudoscalar A, and two charged scalars $H^\pm$. In our model the only locus of CP violation is the CKM matrix. Strong CP violation is absent both at the tree and one-loop levels. We work out the phenomenological constraints on our model, which features flavour-changing neutral Yukawa interactions, showing that the new scalar particles may in some cases be lighter than $500\,\text{GeV}$.

‡pmmferreira@fc.ul.pt
§balio@cftp.tecnico.ulisboa.pt

1   Introduction

Non-perturbative effects in Quantum Chromodynamics (QCD) may lead to P and CP violation, characterized by a parameter θ, in hadronic processes. The experimental upper bound on the electric dipole moment of the neutron necessitates $\theta \lesssim 10^{-9}$.[1] The presence in the Lagrangian of this unnaturally small parameter is known as the 'strong CP problem'.

The angle θ is the sum of two terms, θ_{QCD} and θ_{QFD}. Here, θ_{QCD} is the value of a P- and CP-violating angle in the QCD vacuum, and θ_{QFD} originates in the chiral rotation of the quark fields needed to render the quark masses real and positive. Let p and n denote the three up-type quarks and the three down-type quarks, respectively, in a weak basis. Let the mass terms of those quarks be given by

$$\mathcal{L}_{\mathrm{mass}} = -\bar{p}_L M_p p_R - \bar{n}_L M_n n_R + \mathrm{H.c.}, \tag{1}$$

where M_p and M_n are 3×3 matrices in flavour space. Then, $\theta_{\mathrm{QFD}} = \arg\det\left(M_p M_n\right)$.

There are two general approaches to solving the strong CP problem. In the first approach it is claimed that θ has no significance or physical consequences; theories with different values of θ are equivalent and one may set θ to zero without loss of generality. This may happen either because one of the quarks is massless[2] or because of the presence in the theory of a Peccei–Quinn symmetry [3]; there are also claims that QCD dynamics itself cures the strong CP problem.[3] The second approach, which we shall follow, acknowledges the strong CP problem and tries to find some symmetry that naturally leads to the smallness of θ. One firstly assumes the dimension-four part of the Lagrangian to be either CP-symmetric or P-symmetric; this assumption sets θ_{QCD} to zero. The CP or P symmetry must be either softly or spontaneously broken; one performs this breaking in such a way that θ_{QFD} turns out to be zero at the tree level, because of some peculiar form of M_p and M_n. Still, it is difficult to avoid loop contributions to θ_{QFD} arising from the quark self-energies Σ; they add to the tree-level mass matrices M and then

$$\arg\det\left(M + \Sigma\right) \approx \mathrm{Im}\left[\mathrm{tr}\left(M^{-1}\Sigma\right)\right] \tag{2}$$

is in general nonzero. Artful models are able to obtain $\mathrm{Im}\left[\mathrm{tr}\left(M_p^{-1}\Sigma_p\right)\right] + \mathrm{Im}\left[\mathrm{tr}\left(M_n^{-1}\Sigma_n\right)\right]$ equal to zero at the one-loop level and sometimes even at the two-loop level.

There are various ways to achieve quark mass matrices displaying $\arg\det\left(M_p M_n\right) = 0$. Most of those ways, collectively known as Barr–Nelson-type models, employ extra quarks. There are also many models for solving the strong CP problem that use extra gauge symmetries, especially the left–right symmetry $SU(2)_{\mathrm{L}} \times SU(2)_{\mathrm{R}} \times U(1)_{B-L}$. In this paper we propose a simple extension of the Standard Model (SM), with gauge group $SU(2)_{\mathrm{L}} \times U(1)$ and without any extra fermions, that partially solves the strong CP problem. Our model is a two-Higgs-doublet model (2HDM) [5].

In a 2HDM the quark Yukawa Lagrangian is

$$\mathcal{L}_{\mathrm{Yukawa}} = -\sum_{j,k=1}^{3}\sum_{a=1}^{2} \bar{Q}_{Lj}\left[\Phi_a\left(\Gamma_a\right)_{jk} n_{Rk} + \tilde{\Phi}_a\left(\Delta_a\right)_{jk} p_{Rk}\right] + \mathrm{H.c.} \tag{3}$$

---

[1]For a recente estimate of the maximum possible value of θ, see ref. [1].
[2]For a recent speculation that some quarks may be massless, see ref. [2].
[3]For a recent instance of such a claim, see ref. [4].

where $\Phi_a = \begin{pmatrix} \phi_a^+, & \phi_a^0 \end{pmatrix}^T$ and $\tilde{\Phi}_a = \begin{pmatrix} \phi_a^{0*}, & -\phi_a^- \end{pmatrix}^T$ for $a = 1, 2$ are scalar doublets of $SU(2)_\mathrm{L}$. Furthermore, $\bar{Q}_{Lj} = \begin{pmatrix} \bar{p}_{Lj}, & \bar{n}_{Lj} \end{pmatrix}$, and the Γ_a and Δ_a are four 3×3 matrices in flavour space containing the Yukawa coupling constants. We expand the scalar doublets as

$$\Phi_a = e^{i\aleph_a} \begin{pmatrix} \phi_a^+ \\ (v_a + \rho_a + i\eta_a)/\sqrt{2} \end{pmatrix}, \tag{4}$$

where $v_a \exp(i\aleph_a)/\sqrt{2} = \langle 0 | \phi_a^0 | 0 \rangle$ and the v_a are non-negative real by definition. We define $v = \sqrt{v_1^2 + v_2^2} = 2m_W/g = 246\,\mathrm{GeV}$ and $\tan\beta \equiv v_2/v_1$; then,

$$\frac{v_1}{v} = \cos\beta, \quad \frac{v_2}{v} = \sin\beta, \tag{5}$$

where the angle β is in the first quadrant. There is one physical pseudoscalar A and one unphysical (Goldstone boson) pseudoscalar G^0:

$$\begin{pmatrix} G^0 \\ A \end{pmatrix} = \begin{pmatrix} c_\beta & s_\beta \\ s_\beta & -c_\beta \end{pmatrix} \begin{pmatrix} \eta_1 \\ \eta_2 \end{pmatrix}. \tag{6}$$

(From now on, $s_\xi \equiv \sin\xi$ and $c_\xi \equiv \cos\xi$ for any needed angle ξ.) There is a pair of physical charged scalars $H^\pm$ and a pair of unphysical (Goldstone bosons) charged scalars $G^\pm$:

$$\begin{pmatrix} G^\pm \\ H^\pm \end{pmatrix} = \begin{pmatrix} c_\beta & s_\beta \\ s_\beta & -c_\beta \end{pmatrix} \begin{pmatrix} \phi_1^\pm \\ \phi_2^\pm \end{pmatrix}. \tag{7}$$

There are two physical neutral scalars h and H:

$$\begin{pmatrix} h \\ H \end{pmatrix} = \begin{pmatrix} s_\alpha & -c_\alpha \\ -c_\alpha & -s_\alpha \end{pmatrix} \begin{pmatrix} \rho_1 \\ \rho_2 \end{pmatrix}. \tag{8}$$

The neutral scalar h is chosen to coincide with the LHC-observed particle with mass $125\,\mathrm{GeV}$. In our specific 2HDM there are softly-broken CP and $\mathbb{Z}_3$ symmetries such that h and H do *not* mix with A. The interaction Lagrangian between a scalar and a pair of gauge bosons is

$$\begin{aligned} \mathcal{L}_{SVV} &= \frac{g}{v} \left(m_W W_\xi^- W^{\xi+} + \frac{m_Z}{2c_{\theta_w}} Z_\xi Z^\xi \right) (v_1 \rho_1 + v_2 \rho_2) \tag{9a} \\ &= -g \left(m_W W_\xi^- W^{\xi+} + \frac{m_Z}{2c_{\theta_w}} Z_\xi Z^\xi \right) (h s_{\beta-\alpha} + H c_{\beta-\alpha}), \tag{9b} \end{aligned}$$

where θ_w is Weinberg's angle. Because of the LHC data we now know that $|s_{\beta-\alpha}| \approx 1$.

The quark mass matrices are

$$\begin{aligned} M_n &= \frac{v_1 e^{i\aleph_1}\Gamma_1 + v_2 e^{i\aleph_2}\Gamma_2}{\sqrt{2}}, \tag{10a} \\ M_p &= \frac{v_1 e^{-i\aleph_1}\Delta_1 + v_2 e^{-i\aleph_2}\Delta_2}{\sqrt{2}}. \tag{10b} \end{aligned}$$

Let the unitary matrices $U_{L,R}^{n,p}$ bi-diagonalize M_n and M_p as

$$U_L^{n\dagger} M_n U_R^n = M_d \equiv \mathrm{diag}(m_d, \ m_s, \ m_b), \tag{11a}$$

3

$$U_L^{p\dagger} M_p U_R^p \;=\; M_u \equiv \mathrm{diag}\left(m_u,\; m_c,\; m_t\right). \tag{11b}$$

The CKM matrix is

$$V = U_L^{p\dagger} U_L^n. \tag{12}$$

We define

$$N_n \;=\; \frac{v_2 e^{i\aleph_1}\Gamma_1 - v_1 e^{i\aleph_2}\Gamma_2}{\sqrt{2}}, \tag{13a}$$

$$N_p \;=\; \frac{v_2 e^{-i\aleph_1}\Delta_1 - v_1 e^{-i\aleph_2}\Delta_2}{\sqrt{2}}, \tag{13b}$$

and

$$N_d \;=\; U_L^{n\dagger} N_n U_R^n, \tag{14a}$$

$$N_u \;=\; U_L^{p\dagger} N_p U_R^p. \tag{14b}$$

Then, the Yukawa interactions in the physical basis are given by

$$\mathcal{L}_{\mathrm{physical}} \;=\; \frac{iA}{v}\, \bar{u}\left(N_u P_R - N_u^\dagger P_L\right) u \tag{15a}$$

$$+\frac{iA}{v}\, \bar{d}\left(N_d^\dagger P_L - N_d P_R\right) d \tag{15b}$$

$$+\frac{h}{v}\, \bar{u}\left[\left(s_{\beta-\alpha}M_u - c_{\beta-\alpha}N_u^\dagger\right) P_L + \left(s_{\beta-\alpha}M_u - c_{\beta-\alpha}N_u\right) P_R\right] u \tag{15c}$$

$$+\frac{h}{v}\, \bar{d}\left[\left(s_{\beta-\alpha}M_d - c_{\beta-\alpha}N_d^\dagger\right) P_L + \left(s_{\beta-\alpha}M_d - c_{\beta-\alpha}N_d\right) P_R\right] d \tag{15d}$$

$$+\frac{H}{v}\, \bar{u}\left[\left(c_{\beta-\alpha}M_u + s_{\beta-\alpha}N_u^\dagger\right) P_L + \left(c_{\beta-\alpha}M_u + s_{\beta-\alpha}N_u\right) P_R\right] u \tag{15e}$$

$$+\frac{H}{v}\, \bar{d}\left[\left(c_{\beta-\alpha}M_d + s_{\beta-\alpha}N_d^\dagger\right) P_L + \left(c_{\beta-\alpha}M_d + s_{\beta-\alpha}N_d\right) P_R\right] d \tag{15f}$$

$$+\frac{\sqrt{2}H^+}{v}\, \bar{u}\left(N_u^\dagger V P_L - V N_d P_R\right) d \tag{15g}$$

$$+\frac{\sqrt{2}H^-}{v}\, \bar{d}\left(V^\dagger N_u P_R - N_d^\dagger V^\dagger P_L\right) u, \tag{15h}$$

where $P_L = (1-\gamma_5)/2$ and $P_R = (1+\gamma_5)/2$ are the projectors of chirality. Also, u and d are column vectors subsuming the fields of the physical up-type and down-type quarks, respectively. In equation (15) we have omitted the Yukawa interactions of the Goldstone bosons; they have the same Lagrangian as in the SM.

In this paper we put forward a 2HDM where CP is conserved *in the dimension-four terms* of the Lagrangian, hence $\theta_{\mathrm{QCD}} = 0$, and $\det\left(M_p M_n\right)$ is real both because of CP and because of a $\mathbb{Z}_3$ symmetry. (Another symmetry-furnished 2HDM that also purported to alleviate the strong CP problem was proposed long time ago [6].) Remarkably, our model provides for the absence of strong CP violation even at the one-loop level.

In section 2 we explain our model. In section 3 we demonstrate that strong CP violation vanishes at the one-loop level in our model. Section 4 is devoted to the phenomenological constraints on the model. Section 5 contains the main conclusions of our work. Appendices A, B, and C present some formulas used in the analysis of section 4; appendix D gives a benchmark point for the parameters of the model.

2 The model

Our model is a 2HDM supplemented by the standard CP symmetry and by a $\mathbb{Z}_3$ symmetry. Let $\omega = \exp(2i\pi/3)$, then the $\mathbb{Z}_3$ symmetry reads

$$\Phi_2 \to \omega^2 \Phi_2, \tag{16a}$$

$$Q_{L1} \to \omega^2 Q_{L1}, \quad Q_{L2} \to \omega Q_{L2}, \tag{16b}$$

$$n_{R3} \to \omega n_{R3}, \tag{16c}$$

$$p_{R1} \to \omega p_{R1}, \quad p_{R2} \to \omega p_{R2}. \tag{16d}$$

This represents just a slight change from the $\mathbb{Z}_3$ symmetry of the 2HDM of ref. [7].

Both CP and $\mathbb{Z}_3$ are softly broken by terms in the quadratic part of the scalar potential. Soft breaking of a symmetry consists in that symmetry holding in all the Lagrangian terms of dimension higher than some value, but not holding for the Lagrangian terms of dimension smaller than, or equal to, that value. In our case, both CP and $\mathbb{Z}_3$ hold for terms of dimension four but are broken by terms of dimension two, *viz.* by the terms with coefficient μ_3 in line (17a). In principle, a model with a softly broken symmetry should eventually be justified through an ultraviolet completion, *viz.* a more complete model, with extra fields active at higher energies, which effectively mimics at low energy scales the model with the softly-broken symmetry. Unfortunately, such a ultraviolet completion is often quite difficult to construct explicitly – we attempted such a construction by adding singlet scalar fields to the theory, who would develop vevs at some high scale and then be "integrated out", leaving the desired low energy potential with only two doublets. However, we were unable to build such extensions that left both the CP and $\mathbb{Z}_3$ symmetries intact at low energies – which of course does not mean such an UV completion does not exist. In the absence of any such explicit construction, a softly broken symmetry constitutes a strong, non-trivial assumption. This is, certainly, a weakness of the model in this paper.

The softly broken CP and $\mathbb{Z}_3$ scalar potential is written as

$$V = \mu_1 \, \Phi_1^\dagger \Phi_1 + \mu_2 \, \Phi_2^\dagger \Phi_2 - \mu_3 \left(e^{-i\aleph} \Phi_1^\dagger \Phi_2 + e^{i\aleph} \Phi_2^\dagger \Phi_1 \right) \tag{17a}$$

$$+ \frac{\lambda_1}{2} \left(\Phi_1^\dagger \Phi_1 \right)^2 + \frac{\lambda_2}{2} \left(\Phi_2^\dagger \Phi_2 \right)^2 + \lambda_3 \, \Phi_1^\dagger \Phi_1 \, \Phi_2^\dagger \Phi_2 + \lambda_4 \, \Phi_1^\dagger \Phi_2 \, \Phi_2^\dagger \Phi_1, \tag{17b}$$

where μ_3 is real and positive by definition. The terms with coefficient μ_3 break the symmetry $\mathbb{Z}_3$ softly. The phase $\aleph$ breaks CP softly.

The vacuum expectation values $\langle 0 | \phi_a^0 | 0 \rangle = v_a \exp(i\aleph_a) / \sqrt{2}$ have phases $\aleph_a$ such that $\aleph_2 - \aleph_1 = \aleph$ offsets the phase $-\aleph$ of the term $-\mu_3 e^{-i\aleph} \Phi_1^\dagger \Phi_2$ of the scalar potential. Thus, there is one gauge-invariant vacuum phase that offsets one phase in the potential, with the consequence that the potential of the physical scalar fields is CP-invariant, in particular there is no mixing between the scalars h and H and the pseudoscalar A. The stationarity equations for the vacuum are

$$\mu_1 v_1^2 + \frac{\lambda_1}{2} v_1^4 = \mu_2 v_2^2 + \frac{\lambda_2}{2} v_2^4 = \mu_3 v_1 v_2 - \frac{\lambda_3 + \lambda_4}{2} v_1^2 v_2^2. \tag{18}$$

Referring to equation (4) and defining

$$T_a = \frac{\rho_a^2 + \eta_a^2}{2} + \phi_a^- \phi_a^+ \tag{19}$$

for $a = 1, 2$, the potential is then

$$V = -\frac{\lambda_1 v_1^4 + \lambda_2 v_2^4}{8} - \frac{\lambda_3 + \lambda_4}{4} v_1^2 v_2^2 \tag{20a}$$

$$+ \mu_3 \left(\frac{v_2}{v_1} T_1 + \frac{v_1}{v_2} T_2 - \rho_1 \rho_2 - \eta_1 \eta_2 - \phi_1^- \phi_2^+ - \phi_2^- \phi_1^+ \right) \tag{20b}$$

$$+ \sum_{a=1}^{2} \frac{\lambda_a}{2} \left(v_a \rho_a + T_a \right)^2 + (\lambda_3 + \lambda_4) \left(v_1 \rho_1 + T_1 \right) \left(v_2 \rho_2 + T_2 \right) \tag{20c}$$

$$- \frac{\lambda_4}{2} \left\{ \left[(v_1 + \rho_1) \phi_2^- - (v_2 + \rho_2) \phi_1^- \right] \left[(v_1 + \rho_1) \phi_2^+ - (v_2 + \rho_2) \phi_1^+ \right] \right. \tag{20d}$$

$$+ \left(\eta_1 \phi_2^- - \eta_2 \phi_1^- \right) \left(\eta_1 \phi_2^+ - \eta_2 \phi_1^+ \right) \tag{20e}$$

$$\left. + i \left(\phi_2^- \phi_1^+ - \phi_1^- \phi_2^+ \right) \left[\eta_1 (v_2 + \rho_2) - \eta_2 (v_1 + \rho_1) \right] \right\}. \tag{20f}$$

The potential (20) is invariant under the CP transformation

$$CP: \quad \begin{cases} \phi_a^- (x) & \to & \exp (i\lambda) \, \phi_a^+ (\bar{x}), \\ \phi_a^+ (x) & \to & \exp (-i\lambda) \, \phi_a^- (\bar{x}), \\ \rho_a (x) & \to & \rho_a (\bar{x}), \\ \eta_a (x) & \to & -\eta_a (\bar{x}), \end{cases} \tag{21}$$

for $a = 1, 2$, where $x = (t, \, \vec{r})$ and $\bar{x} = (t, \, -\vec{r})$. The phase λ in the CP transformation (21) is arbitrary.

The physical potential contains seven parameters $\mu_{1,2,3}$ and $\lambda_{1,2,3,4}$, since the phase $\aleph$ in line (17a) is cancelled out by the vacuum phase. Instead of those seven parameters we will use as input $v = 246 \, \text{GeV}$, $m_h = 125 \, \text{GeV}$, the angles α and β, and the masses m_H of H, m_A of A, and m_{H^+} of $H^\pm$. Then [8],

$$\mu_3 = m_A^2 s_\beta c_\beta, \tag{22a}$$

$$\lambda_1 = \frac{-m_A^2 s_\beta^2 + m_h^2 s_\alpha^2 + m_H^2 c_\alpha^2}{v^2 c_\beta^2}, \tag{22b}$$

$$\lambda_2 = \frac{-m_A^2 c_\beta^2 + m_h^2 c_\alpha^2 + m_H^2 s_\alpha^2}{v^2 s_\beta^2}, \tag{22c}$$

$$\lambda_3 = \frac{2 m_{H^+}^2 - m_A^2}{v^2} + \frac{\left(m_H^2 - m_h^2 \right) s_\alpha c_\alpha}{v^2 s_\beta c_\beta}, \tag{22d}$$

$$\lambda_4 = \frac{2 \left(m_A^2 - m_{H^+}^2 \right)}{v^2}. \tag{22e}$$

In order for the potential to be bounded from below, one must impose the conditions [5]

$$\lambda_1 > 0, \quad \lambda_2 > 0, \quad \lambda_3 > -\sqrt{\lambda_1 \lambda_2}, \quad \lambda_3 + \lambda_4 > -\sqrt{\lambda_1 \lambda_2}. \tag{23}$$

In order to avoid the situation of 'panic vacuum' [8] one must enforce the condition [9]

$$\frac{2 \mu_3}{v_1 v_2} > \lambda_3 + \lambda_4 - \sqrt{\lambda_1 \lambda_2}. \tag{24}$$

The conditions in order for tree-level unitarity not to be violated are

$$|\lambda_1| < 8\pi, \tag{25a}$$
$$|\lambda_2| < 8\pi, \tag{25b}$$
$$|\lambda_3| < 8\pi, \tag{25c}$$
$$|\lambda_3 + \lambda_4| < 8\pi, \tag{25d}$$
$$|\lambda_3 - \lambda_4| < 8\pi, \tag{25e}$$
$$|\lambda_3 + 2\lambda_4| < 8\pi, \tag{25f}$$
$$\left|\lambda_1 + \lambda_2 + \sqrt{(\lambda_1 - \lambda_2)^2 + 4\lambda_4^2}\right| < 16\pi, \tag{25g}$$
$$\left|3\lambda_1 + 3\lambda_2 + \sqrt{9(\lambda_1 - \lambda_2)^2 + 4(2\lambda_3 + \lambda_4)^2}\right| < 16\pi. \tag{25h}$$

Because of the $\mathbb{Z}_3$ symmetry (16), the matrices Γ_a and Δ_a are

$$\Gamma_1 = \begin{pmatrix} 0 & 0 & 0 \\ 0 & 0 & b_1 \\ d_1 & f_1 & 0 \end{pmatrix}, \quad \Gamma_2 = \begin{pmatrix} d_2 & f_2 & 0 \\ 0 & 0 & 0 \\ 0 & 0 & b_2 \end{pmatrix}, \tag{26a}$$

$$\Delta_1 = \begin{pmatrix} 0 & 0 & 0 \\ p_1 & q_1 & 0 \\ 0 & 0 & r_1 \end{pmatrix}, \quad \Delta_2 = \begin{pmatrix} p_2 & q_2 & 0 \\ 0 & 0 & r_2 \\ 0 & 0 & 0 \end{pmatrix}. \tag{26b}$$

The dimensionless numbers b_a, d_a, f_a, p_a, q_a, and r_a ($a = 1, 2$) are real because of the CP symmetry. Clearly,

$$M_n = \frac{1}{\sqrt{2}} \begin{pmatrix} d_2 v_2 e^{i\aleph_2} & f_2 v_2 e^{i\aleph_2} & 0 \\ 0 & 0 & b_1 v_1 e^{i\aleph_1} \\ d_1 v_1 e^{i\aleph_1} & f_1 v_1 e^{i\aleph_1} & b_2 v_2 e^{i\aleph_2} \end{pmatrix}, \tag{27a}$$

$$M_p = \frac{1}{\sqrt{2}} \begin{pmatrix} p_2 v_2 e^{-i\aleph_2} & q_2 v_2 e^{-i\aleph_2} & 0 \\ p_1 v_1 e^{-i\aleph_1} & q_1 v_1 e^{-i\aleph_1} & r_2 v_2 e^{-i\aleph_2} \\ 0 & 0 & r_1 v_1 e^{-i\aleph_1} \end{pmatrix}. \tag{27b}$$

Therefore

$$\det(M_n M_p) = \frac{v_1^4 v_2^2}{8} b_1 (d_1 f_2 - d_2 f_1) r_1 (p_2 q_1 - p_1 q_2) \tag{28}$$

is real, hence $\theta_{\text{QFD}} = 0$. Because of the assumed CP invariance of the quartic part of the Lagrangian, $\theta_{\text{QCD}} = 0$ too. Thus, $\theta = \theta_{\text{QCD}} + \theta_{\text{QFD}} = 0$, i.e. there is no strong CP violation at the tree level.

We now define

$$\beta_a \equiv \arg b_a, \quad \delta_a \equiv \arg d_a, \quad \varphi_a \equiv \arg f_a, \tag{29a}$$
$$\pi_a \equiv \arg p_a, \quad \chi_a \equiv \arg q_a, \quad \varrho_a \equiv \arg r_a, \tag{29b}$$

for $a = 1, 2$; and

$$\Delta\beta \equiv \beta_2 - \beta_1, \quad \Delta\delta \equiv \delta_2 - \delta_1, \quad \Delta\varphi \equiv \varphi_2 - \varphi_1, \tag{30a}$$

7

$$\Delta\pi \equiv \pi_2 - \pi_1, \quad \Delta\chi \equiv \chi_2 - \chi_1, \quad \Delta\varrho \equiv \varrho_2 - \varrho_1. \tag{30b}$$

All the phases in equations (29) and (30) are either 0 or π because $b_a, d_a, \ldots, r_a$ are real. We define the diagonal matrices

$$\begin{align}
X_{Ln} &= \text{diag}\left(1,\ e^{i(2\aleph + \Delta\delta + \Delta\beta)},\ e^{i(\aleph + \Delta\delta)}\right), \tag{31a}\\
X_{Rn} &= \text{diag}\left(e^{i(-\aleph_2 - \delta_2)},\ e^{i(-\aleph_2 - \varphi_2)},\ e^{i(\aleph_1 - 2\aleph_2 - \Delta\delta - \beta_2)}\right), \tag{31b}\\
X_{Lp} &= \text{diag}\left(1,\ e^{i(-\aleph + \Delta\pi)},\ e^{i(-2\aleph + \Delta\pi + \Delta\varrho)}\right), \tag{31c}\\
X_{Rp} &= \text{diag}\left(e^{i(\aleph_2 - \pi_2)},\ e^{i(\aleph_2 - \chi_2)},\ e^{i(2\aleph_2 - \aleph_1 - \Delta\pi - \varrho_2)}\right), \tag{31d}
\end{align}$$

where $\aleph = \aleph_2 - \aleph_1$. We then have

$$X_{Ln} M_n X_{Rn} = \frac{1}{\sqrt{2}}\begin{pmatrix} |d_2 v_2| & |f_2 v_2| & 0 \\ 0 & 0 & |b_1 v_1| \\ |d_1 v_1| & |f_1 v_1|\, e^{i(\Delta\delta - \Delta\varphi)} & |b_2 v_2| \end{pmatrix} \tag{32a}$$

$$\equiv M_n', \tag{32b}$$

$$X_{Lp} M_p X_{Rp} = \frac{1}{\sqrt{2}}\begin{pmatrix} |p_2 v_2| & |q_2 v_2| & 0 \\ |p_1 v_1| & |q_1 v_1|\, e^{i(\Delta\pi - \Delta\chi)} & |r_2 v_2| \\ 0 & 0 & |r_1 v_1| \end{pmatrix} \tag{32c}$$

$$\equiv M_p'. \tag{32d}$$

The matrices M_n' and M_p' are real, therefore they may be bi-diagonalized through real orthogonal matrices O_{Ln}, O_{Rn}, O_{Lp}, and O_{Rp} as

$$O_{Ln} M_n' O_{Rn} = M_d, \quad O_{Lp} M_p' O_{Rp} = M_u. \tag{33}$$

Therefore, in the notation of equations (11),

$$U_L^{n\dagger} = O_{Ln} X_{Ln}, \quad U_R^n = X_{Rn} O_{Rn}, \quad U_L^{p\dagger} = O_{Lp} X_{Lp} \quad U_R^p = X_{Rp} O_{Rp}. \tag{34}$$

The CKM matrix is then

$$V = O_{Lp} \times \text{diag}\left(1,\ e^{i(-3\aleph + \Delta\pi - \Delta\delta - \Delta\beta)},\ e^{i(-3\aleph + \Delta\pi - \Delta\delta + \Delta\varrho)}\right) \times O_{Ln}^T. \tag{35}$$

One sees that the CKM matrix is *complex* because of the presence of the phase $3\aleph$.

When we compute the matrices N_p and N_n defined in equations (13), we find that

$$X_{Ln} N_n X_{Rn} = \frac{1}{\sqrt{2}}\begin{pmatrix} -|d_2 v_1| & -|f_2 v_1| & 0 \\ 0 & 0 & |b_1 v_2| \\ |d_1 v_2| & |f_1 v_2|\, e^{i(\Delta\delta - \Delta\varphi)} & -|b_2 v_1| \end{pmatrix} \tag{36a}$$

$$\equiv N_n', \tag{36b}$$

$$X_{Lp} N_p X_{Rp} = \frac{1}{\sqrt{2}}\begin{pmatrix} -|p_2 v_1| & -|q_2 v_1| & 0 \\ |p_1 v_2| & |q_1 v_2|\, e^{i(\Delta\pi - \Delta\chi)} & -|r_2 v_1| \\ 0 & 0 & |r_1 v_2| \end{pmatrix} \tag{36c}$$

$$\equiv N_p', \tag{36d}$$

and then, from equations (14),

$$N_d = O_{Ln} N'_n O_{Rn}, \quad N_u = O_{Lp} N'_p O_{Rp}. \tag{37}$$

The matrices N_d and N_u are *real*.

Thus, in our model

1. The CKM matrix is complex.

2. The matrices N_u and N_d are real.

3. There is one pseudoscalar A that does not mix with the scalars h and H.

4. There is no CP violation in the cubic and quartic interactions of the scalars.

In our model CP violation is located solely in the CKM matrix and originates entirely in the phase $3\aleph$. This is the same that happened in the model of ref. [7]; however, in that model there was strong CP violation, while in the present model strong CP violation is absent at the tree level.

3   No strong CP violation at the one-loop level

At one-loop level the diagonal and real quark mass matrices M_q (where q may be either u or d) get corrected by self energy diagrams: $M_q \to M_q + \Sigma_q$. If the diagonal elements of Σ_q are complex, then $\text{Im}\left[\text{tr}\left(M_q^{-1}\Sigma_q\right)\right]$ may be nonzero and strong CP violation may arise.

In our model there are no complex phases except in the CKM matrix. Since the matrices N_q are real, and since the scalars h and H do not mix with the pseudoscalar A, the Σ_q generated through the emission and reabsorption (E&R) by the quarks of either h or H or A are real, hence innocuous. The same happens with the Σ_q generated through the E&R of Z^0 gauge bosons. On the other hand, diagrams with the E&R of $W^\pm$ gauge bosons do not generate mass renormalization (they just produce wavefunction renormalization), since the coupling of $W^\pm$ to the quarks is purely left-handed. Therefore, the only diagrams where the complex matrix V arises, and might produce complex Σ_q, are the ones with E&R of charged scalars $H^\pm$.

The Yukawa interactions of the charged scalars are given by lines (15g) and (15h). They contain two complex matrices, $X \equiv N_u^\dagger V$ and $Y \equiv V N_d$. The one-loop self-energy of an up-type quark u_α caused by the E&R of H^+ and a down-type quark d_j is

$$-i\Sigma_\alpha(p) = \frac{2}{v^2} \mu^{4-d} \int \frac{\mathrm{d}^d k}{(2\pi)^d} \frac{1}{k^2 - m_j^2} \frac{1}{(k-p)^2 - m_{H^+}^2} \tag{38a}$$

$$\times (X_{\alpha j} P_L - Y_{\alpha j} P_R)(\slashed{k} + m_j)\left(X_{j\alpha}^\dagger P_R - Y_{j\alpha}^\dagger P_L\right) \tag{38b}$$

$$= \frac{2}{v^2} \mu^{4-d} \int \frac{\mathrm{d}^d k}{(2\pi)^d} \int_0^1 \mathrm{d}x \, \frac{1}{\left(k^2 - \Delta_j\right)^2} \tag{38c}$$

$$\times \left(x\,|X_{\alpha j}|^2\,\slashed{p}P_R + x\,|Y_{\alpha j}|^2\,\slashed{p}P_L - X_{\alpha j} m_j Y_{j\alpha}^\dagger P_L - Y_{\alpha j} m_j X_{j\alpha}^\dagger P_R\right), \tag{38d}$$

9

where
$$\Delta_j = p^2 x^2 + \left(-p^2 + m_{H^+}^2 - m_j^2\right) x + m_j^2 \tag{39}$$
and we perform the computation in a space–time of dimension d. Thus, the only potentially complex part of the self-energy is
$$\Sigma_\alpha \left(\not{p} \to 0\right) = -\int_0^1 \mathrm{d}x \, \frac{X_{\alpha j} m_j Y_{j\alpha}^\dagger P_L + Y_{\alpha j} m_j X_{j\alpha}^\dagger P_R}{8\pi^2 v^2} \left(\frac{2}{4-d} - \gamma - \ln \frac{\Delta_j}{4\pi\mu^2}\right), \tag{40}$$
where γ is Euler–Mascheroni's constant. One must sum the expression in the right-hand side of equation (40) over the flavour j of the quark d_j.

The one-loop value of the strong-CP parameter θ is $\mathrm{Im}\left[\mathrm{tr}\left(M_u^{-1}\Sigma_u + M_d^{-1}\Sigma_d\right)\right]$. The diagonal matrix elements of $M_u^{-1}\Sigma_u$ are $m_\alpha^{-1}\Sigma_\alpha\left(\not{p}\to 0\right)$. Now,

$$\sum_\alpha \frac{X_{\alpha i} Y_{j\alpha}^\dagger}{m_\alpha} = \sum_\alpha \left(N_d^\dagger V^\dagger\right)_{j\alpha} \frac{1}{m_\alpha} \left(N_u^\dagger V\right)_{\alpha i} \tag{41a}$$

$$= \left(N_d^\dagger V^\dagger M_u^{-1\dagger} N_u^\dagger V\right)_{ji} \tag{41b}$$

$$= \left(U_R^{n\dagger} N_n^\dagger M_p^{-1\dagger} N_p^\dagger U_L^n\right)_{ji}. \tag{41c}$$

Therefore,

$$\sum_{\alpha,j} \frac{X_{\alpha j} m_j Y_{j\alpha}^\dagger f\left(m_j^2\right)}{m_\alpha} = \sum_j f\left(m_j^2\right) m_j \left(U_R^{n\dagger} N_n^\dagger M_p^{-1\dagger} N_p^\dagger U_L^n\right)_{jj} \tag{42a}$$

$$= \mathrm{tr}\left[U_L^n f\left(M_d M_d^\dagger\right) M_d U_R^{n\dagger} N_n^\dagger M_p^{-1\dagger} N_p^\dagger\right] \tag{42b}$$

$$= \mathrm{tr}\left[f\left(M_n M_n^\dagger\right) M_n N_n^\dagger M_p^{-1\dagger} N_p^\dagger\right]. \tag{42c}$$

One easily finds that, in our model, both matrices $M_n M_n^\dagger$ and $M_n N_n^\dagger M_p^{-1\dagger} N_p^\dagger$, and all of their products too, have a structure of phases of the form

$$\begin{pmatrix} 0 & 2\aleph & \aleph \\ -2\aleph & 0 & -\aleph \\ -\aleph & \aleph & 0 \end{pmatrix}, \tag{43}$$

where $\aleph = \aleph_2 - \aleph_1$. Therefore, the diagonal matrix elements of $f\left(M_n M_n^\dagger\right) M_n N_n^\dagger M_p^{-1\dagger} N_p^\dagger$, and hence its trace, are real, no matter what the function f is.

In this way we have demonstrated that $\mathrm{tr}\left(M_u^{-1}\Sigma_u\right)$ is real. In a similar way one may show that $\mathrm{tr}\left(M_d^{-1}\Sigma_d\right)$ is also real, hence strong CP violation vanishes at the one-loop level in our model.

4 Phenomenological analysis of the model

4.1 Constraints

We proceed to analyse how our model conforms to the experimental results. The model has tree-level flavour-changing neutral currents (FCNC) coupling to the scalars, so there

is a wealth of flavour-physics observables that need to be taken into account whilst performing a fit of the model to the experimental data. Our procedure involves a global fit of the model's parameters, simultaneously requiring compliance with the theoretical and experimental bounds from the gauge, scalar, and fermionic sectors.

One may rotate the right-handed quarks n_{R1} and n_{R2} between themselves in such a way that the entry f_2 of the Yukawa-coupling matrix Γ_2 becomes zero. Similarly, one may rotate p_{R1} and p_{R2} so that q_2 becomes zero.[4,5] We use as input the ten entries b_1, d_1, f_1, b_2, d_2, p_1, q_1, r_1, p_2, and r_2 (f_2 and q_2 are set to zero) of the Yukawa-coupling matrices (26), allowing those entries to be either positive or negative. We further input the CP-violating phase $\aleph$. We fit these eleven parameters in order to reproduce the quark masses [11][6]

$$
\begin{align}
m_u &= (2.2 \pm 2 \times 0.6)\,\text{MeV}, \tag{44a}\\
m_d &= (4.7 \pm 2 \times 0.5)\,\text{MeV}, \tag{44b}\\
m_s &= (96 \pm 2 \times 8)\,\text{MeV}, \tag{44c}\\
m_c &= (1.28 \pm 0.03)\,\text{GeV}, \tag{44d}\\
m_b &= (4.18 \pm 0.04)\,\text{GeV}, \tag{44e}\\
m_t &= (173.2 \pm 0.6)\,\text{GeV}, \tag{44f}
\end{align}
$$

and the CKM-matrix observables [11]

$$
\begin{align}
|V_{us}| &= 0.2243 \pm 0.0005, \tag{45a}\\
|V_{cb}| &= 0.0422 \pm 0.0008, \tag{45b}\\
|V_{ub}| &= 0.00394 \pm 0.00036, \tag{45c}\\
\gamma \equiv \arg\left(-\frac{V_{ud}V_{ub}^*}{V_{cd}V_{cb}^*}\right) &= (73.5 \pm 5.5)^\circ. \tag{45d}
\end{align}
$$

We furthermore input $\tan\beta = v_2/v_1$. We compute the matrices N_n' and N_p' through equations (36), and the matrices N_d and N_u through equations (37). Finally, we input α and get to know $\mathcal{L}_{\text{physical}}$ in equation (15).[7]

In the scalar potential (17) there are seven independent parameters $\mu_{1,2,3}$ and $\lambda_{1,2,3,4}$. We input instead the seven observables

1. $v = \sqrt{v_1^2 + v_2^2} = 246\,\text{GeV}$, which produces the correct masses for the electroweak gauge bosons $W^\pm$ and Z^0;

2. the lightest CP-even-scalar mass $m_h = 125\,\text{GeV}$, corresponding to the Higgs boson observed at the LHC;

---

[4]Notice that n_{R1} and n_{R2} transform in the same way under the $\mathbb{Z}_3$ symmetry (16), and p_{R1} and p_{R2} also transform in the same way under that symmetry.

[5]With $f_2 = q_2 = 0$, the phases $\Delta\varphi$ and $\Delta\chi$ in equations (30) become meaningless. That has no impact on our reasonings, in particular the matrix V in equation (35) does not depend on those phases.

[6]We have doubled the uncertainty intervals quoted in ref. [11] for the masses of the light quarks u, d, and s; we have done this because of the large theoretical indefinition, due to QCD considerations, as to what exactly should be interpreted as the value of those masses.

[7]The angle α may be restricted to lie either in the first quadrant or in the fourth quadrant [5].

3. the angle $\beta = \arctan(v_2/v_1)$;

4. the angle α;

5. the remaining scalar masses—m_H of the second CP-even scalar, m_A of the pseudoscalar, and m_{H^+} of the charged scalar.

The last five parameters must be found through the fitting procedure. We have constrained m_{H^+} to be larger than $100\,\text{GeV}$ and m_H and m_A to be larger than $130\,\text{GeV}$. We have furthermore assumed all three masses to be smaller than $1.2\,\text{TeV}$; values of the masses larger than $1.2\,\text{TeV}$ would certainly be allowed by the fitting procedure.

The quartic couplings of the model are determined via equations (22). We check that the scalar potential is bounded from below, that it does not have a panic vacuum, and that it satisfies unitarity, *viz.* we check conditions (23, 24, 25). The constraints from the electroweak oblique parameters S and T are also imposed, by using the expressions for the 2HDM in refs. [12, 13].

We will now go into detail about the further constraints that we have imposed.

- We implement the $b \to s\gamma$ bound described in appendix A, including the contributions from both the neutral and the charged scalars.

- The most relevant bounds on the off-diagonal entries of the matrices N_d and N_u come from flavour-physics observables, specifically the K, B_d, B_s, and D neutral-meson mass differences, and the CP-violating parameter ϵ_K. We detail the computation of those quantities, and the requirements on them that we use in our fit, in appendix B.

- The $Z \to b\bar{b}$ constraints described in appendix C are also taken into account. In this case we use only the charged-scalar contributions; the neutral-scalar ones should be negligible.

- For the regions of parameter space where $m_t > m_q + m_{H^+}$, q being a down-type quark, or where $m_t > m_q + m_S$, q being either c or u and S being either h or H or A, we require that the branching ratio for each of the kinematically viable $t \to light\ quark + scalar$ decays be smaller than 5×10^{-3}, in accordance with the current results on FCNC top decays and on the total top-quark width [11].

- In order that the scalar h of our model complies with the observational data from the LHC—it should be SM-like in its behaviour—we require that its couplings to the electroweak gauge bosons and to the top and bottom quarks do not deviate significantly from the SM expectations. We achieve this by focusing on the coupling modifiers κ_X defined as $g_{hZZ} = \kappa_Z\, g_{hZZ}^{\text{SM}}$, $g_{hWW} = \kappa_W\, g_{hWW}^{\text{SM}}$, $g_{ht\bar{t}} = \kappa_t\, g_{ht\bar{t}}^{\text{SM}}$, and $g_{hb\bar{b}} = \kappa_b\, g_{hb\bar{b}}^{\text{SM}}$. In our model $\kappa_Z = \kappa_W \equiv \kappa_V$ and

$$\kappa_V = s_{\beta-\alpha}, \quad \kappa_t = s_{\beta-\alpha} - \frac{c_{\beta-\alpha}\,(N_u)_{33}}{m_t}, \quad \kappa_b = s_{\beta-\alpha} - \frac{c_{\beta-\alpha}\,(N_d)_{33}}{m_b}, \quad (46)$$

cf. equations (15c) and (15d). In the first stage of the fit we constrain these couplings to obey $0.8 \leq \kappa_V \leq 1$, $0.8 \leq \kappa_t \leq 1.2$, and $0.8 \leq |\kappa_b| \leq 1.2$,[8,9] in order to roughly reproduce the LHC results. A second stage of the analysis further constrains these couplings, as detailed below.

A numerical scan of the parameter space of the model, in both the scalar and Yukawa sectors, was performed to discover points that obey all the constraints described above. It must be stressed that we have introduced nowhere in our scan a 'no-fine-tuning' assumption: we have tolerated any set of input values that led to the right outputs, even if either the input values or any intermediate computations displayed either 'fine-tunings' or 'unnatural cancelations'. Strong fine-tunings are often required in order to fit the D-meson mass difference constraint whenever m_H and m_A are not very high; for the other constraints, fine-tunings are at most moderate and do not occur at all for many points in our fit. As a matter of fact, even for the D-meson mass difference, there are many choices of parameters for which no fine-tuning is necessary and one of the scalars has relatively low mass; one such case is presented in appendix D.

With those points we have proceeded to compute the LHC production cross sections of the neutral scalars in the model, using the software `SusHI` [16, 17] to include the NNLO QCD corrections. We have limited ourselves to the gluon–gluon production process, which is the dominant one in the LHC environment. Regarding the vector boson-fusion process, no differences will occur in this model *vis a vis* the usual 2HDM, as the couplings of the scalars to the gauge bosons are the same in both models.

The results for h are expressed in terms of the ratios

$$\mu_X = \frac{\sigma\,(pp \to h)\ \mathrm{BR}\,(h \to X)}{\sigma^{\mathrm{SM}}\,(pp \to h)\ \mathrm{BR}^{\mathrm{SM}}\,(h \to X)}, \tag{47}$$

where X may be either $Z^0 Z^0$, $W^+ W^-$, $b\bar{b}$, $\tau\bar{\tau}$, or $\gamma\gamma$. The value $\mu_X = 1$ indicates exact SM-like behaviour. We require that all the μ_X be within 20% of 1, which is a fair description of the current LHC results, taking into account the uncertainties. With this imposition, the ranges of variation of $\kappa_V = s_{\beta-\alpha}$, κ_t, and κ_b become much smaller than initially allowed in the fit: we obtain $0.929 \leq \kappa_V \leq 1$ and $0.952 \leq \{\kappa_t, \kappa_b\} \leq 1.04$. For comparison, we will also present results for the tighter constraint $|\mu_X - 1| < 0.1$.

In principle, we should also consider the leptons. The $\mathbb{Z}_3$ symmetry in the quark sector must be extended to the leptonic sector. Since flavour violation with leptons is much more constrained than with quarks, the best choice would be to extend $\mathbb{Z}_3$ to the leptonic sector in a way identical to the flavour-preserving 2HDMs, allowing only one of the two doublets Φ_a to couple to the leptons and give them mass. We would then have have two possibilities for the couplings of the scalars to the charged leptons—either Φ_1 couples to the charged leptons or Φ_2 does. The coupling modifier $\kappa_\tau = g_{h\tau\bar{\tau}} / g_{h\tau\bar{\tau}}^{\mathrm{SM}}$ is given by

$$\kappa_\tau = \frac{\cos\alpha}{\sin\beta} \quad \text{and} \quad \kappa_\tau = -\frac{\sin\alpha}{\cos\beta} \tag{48}$$

---

[8]Notice that we allow the possibility of a 'wrong-sign regime' [14, 15] in the bottom-quark coupling. However, the combination of cuts applied to the model ends up not allowing for that regime.

[9]Notice that κ_V and κ_t must have the same sign, otherwise one would expect a huge variation in the h diphoton width, in disagreement with the SM-like observed values.

for the first and second choices, respectively. For definiteness, in our fit we have adopted the second option in equation (48), *viz.* we have imposed

$$0.8 < \left| \frac{\sin \alpha}{\cos \beta} \right| < 1.2 \tag{49}$$

to the points in our fit. However, since the extension of our model to the leptonic sector is largely arbitrary, we have refrained from taking into account any other constraints on our model that might arise from processes involving leptons. We point out, though, that flavour-changing constraints from processes like $K_L \to \mu^+ \mu^-$ or $B_s \to \mu^+ \mu^-$ may pose serious challenges to our model.

4.2   General results

The bounds on the scalar sector—unitarity, oblique parameters, and vacuum stability—produce the same contraints on the model's parameters than those found in the usual version of the 2HDM. On the other hand, since the symmetry that we are considering affects in a non-trivial way the quark Yukawa matrices, there are major differences relative to other 2HDMs when the flavour-physics bounds are imposed. The flavour constraints from meson observables and from the top-quark FCNC decays and total width, previously described, constrain severely the magnitudes of the off-diagonal elements of the matrices N_u and N_d. Our fit achieves to keep FCNC under control even with extra scalars of *"low"* masses—H and A may have masses below $500 \,\mathrm{GeV}$. This is in contrast with the often-made assumption that models with tree-level FCNC imply masses above $1 \,\mathrm{TeV}$; this had already been shown not to necessarily apply in the previous version of the current model [7]. In ref. [18] it has been argued that contributions from the scalar and pseudoscalar particles (H and A, respectively) to FCNC meson observables tend to cancel each other; we have explicitly observed that, for many points in our fit (*cf.* the point given in appendix D), the arguments of ref. [18] apply, and this is the reason why masses of the extra scalars lower than $1 \,\mathrm{TeV}$ are possible.

One consequence of the present model is the fact that the scalar h, which we have taken to be the $125 \,\mathrm{GeV}$ state observed at the LHC, has tree-level FCNCs, as indicated by its Yukawa interactions in lines (15c) and (15d). Thus, unlike in the (tree-level) SM, h has the possibility of FCNC decays to final states $s\bar{b}$, $d\bar{b}$, $d\bar{s}$, $u\bar{c}$, and their charge-conjugate states. However, for all the points resulting from our fit, these decays are extremely suppressed—the sum of the branching ratios for all of them being at most 2×10^{-6} but usually much lower. Therefore, in our model the FCNC decays of the $125 \,\mathrm{GeV}$-particle are impossible to observe at the LHC, and almost certainly even at future $e^+ e^-$ colliders such as the ILC; the existence of those decays has no measurable impact on the phenomenology of the scalar h. The FCNC also raise the possibility of alternative production mechanisms for h, such as $d\bar{s} \to h$ or $u\bar{c} \to h$; such production channels would be favoured by larger proton PDFs relatively to the SM production mechanism $b\bar{b} \to h$. However, once again these FCNC processes are found to be extremely small in our fit. According to (15c) and (15d), all the FCNC h interactions are suppressed by their proportionality to $c_{\beta-\alpha}$, which is required to be quite small by the SM-like behaviour of the $125 \,\mathrm{GeV}$ scalar h, by the ratio between a light-quark mass and $v = 246 \,\mathrm{GeV}$, and, sometimes, by the smallish off-diagonal N_d and N_u matrix elements induced by compliance with meson-physics bounds.
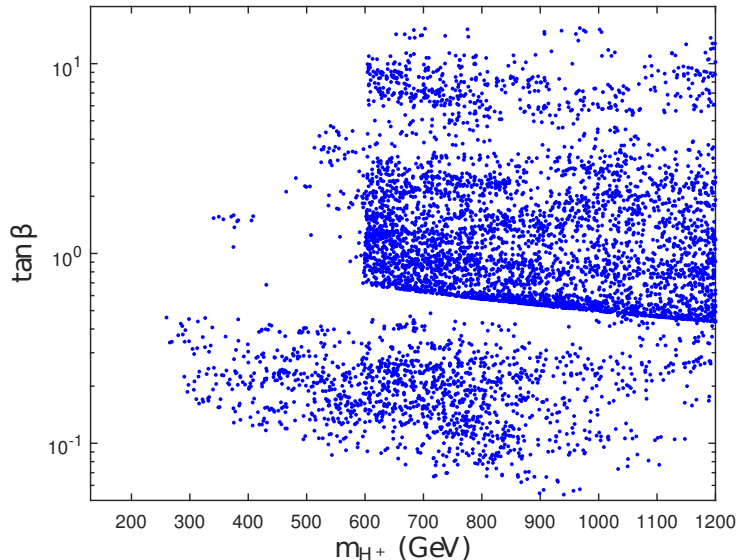
14

Figure 1: v_2/v_1 *versus* the charged-Higgs mass for the parameter-space points that survived all the theoretical and experimental constraints.

In fig. 1 we show the points generated by our fit, displayed on the $\tan\beta$–m_{H^+} plane. (The observed low density of points is merely a consequence of the difficulty in achieving good fits—further searches would yield more points and fill many more regions in the plot; lack of points in some areas has no physical meaning, it is just an artifact of the limited parameter space scan.) A clear conclusion from fig. 1 is that $1/20 < \tan\beta < 20$ in our model[10]; this is mainly a consequence of the $b \to s\gamma$ bounds and, to a lesser degree, of the $Z \to b\bar{b}$ bounds. One also sees in fig. 1 that values of the charged-scalar mass as low as $130\,\mathrm{GeV}$ are easily attained; this is in stark contrast with the findings for the type II 2HDM, where a lower bound on m_{H^+} of roughly $580\,\mathrm{GeV}$ exists. Unlike in the usual type-I and type-II 2HDMs, in our model the quark mass matrices do not emerge from the Yukawa couplings to a single scalar doublet, but rather from the couplings to both Φ_1 and Φ_2. As such, although we employ the standard definition $\tan\beta = v_2/v_1$, the usual wisdom about the values of this parameter does not apply.

The matrices N_u and N_d also exist in the usual flavour-preserving 2HDMs, but there they are diagonal and proportional to the quark mass matrices. In fact, in the type-I 2HDM

$$N_u = -\frac{M_u}{\tan\beta}, \quad N_d = -\frac{M_d}{\tan\beta}, \tag{50}$$

whereas in the type-II 2HDM

$$N_u = -\frac{M_u}{\tan\beta}, \quad N_d = M_d \tan\beta. \tag{51}$$

---

[10]As is plain in equations (26), in our model there is a symmetry between the Yukawa couplings of Φ_1 and the ones of Φ_2, so that, for any given t, $\tan\beta = t$ is just as (im)possible to achieve as $\tan\beta = 1/t$. This is in contrast to what happens in the usual 2HDMs types I and II.
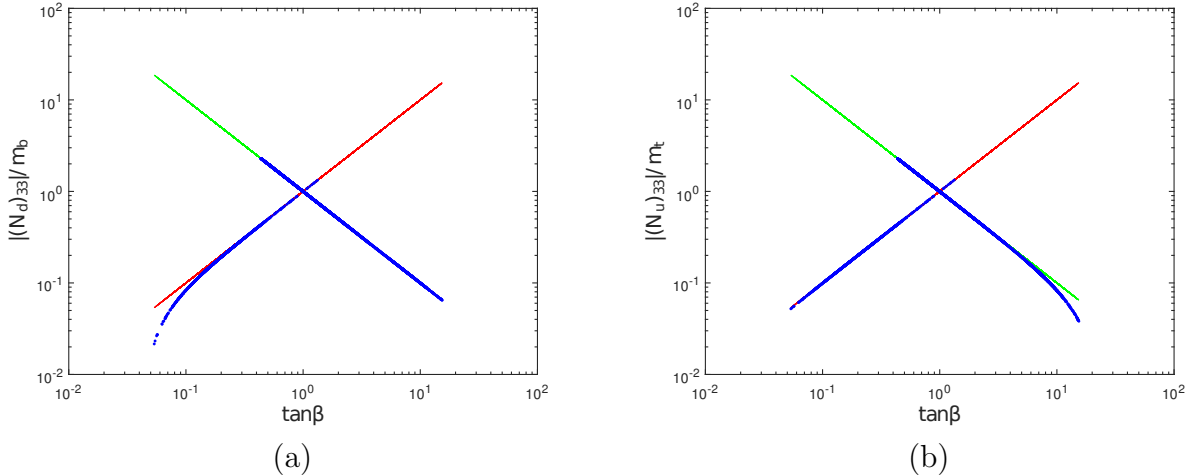
Figure 2: (a) $|(N_d)_{33}|/m_b$ and (b) $|(N_u)_{33}|/m_t$ *versus* $\tan\beta$ for the parameter space points (in blue) which survive all the theoretical and experimental constraints. The green lines correspond to $y = \cot\beta$ and the red lines correspond to $y = \tan\beta$, where y is $|(N_d)_{33}|/m_b$ in (a) and $|(N_u)_{33}|/m_t$ in (b).

Now consider fig. 2, where we have plotted the values of both $|(N_d)_{33}|/m_b$ and $|(N_u)_{33}|/m_t$ as functions of $\tan\beta$. The green line shown in plot (a), upon which many blue points are superimposed, corresponds to $|(N_d)_{33}|/m_b = 1/\tan\beta$, that one would obtain if the model behaved, for the bottom quarks, as a type-I 2HDM. The red line would correspond to type-II behaviour, *viz.* $|(N_d)_{33}|/m_b = \tan\beta$. It appears that, in this model, most regions of parameter space yield either approximate type-I behaviour or approximate type-II behaviour for bottom quarks. Note that, although the blue points appear superimposed on the green and red lines, they are not *exactly* on them—the type-I and type-II behaviours displayed are *approximate* and there are deviations from them, which indeed can be large, as we observe in particular for low values of $\tan\beta$. In fig. 2 (b) we observe the same behaviour for top quarks—most points have either $|(N_u)_{33}|/m_t \approx \tan\beta$ or $|(N_u)_{33}|/m_t \approx \cot\beta$.

From equations (50) it follows that, in the type I 2HDM,

$$\frac{(N_u)_{33}\,m_b}{(N_d)_{33}\,m_t} \tag{52}$$

is equal to one, whereas in the type II 2HDM, from equations (51),

$$-\frac{(N_u)_{33}\,(N_d)_{33}}{m_t m_b} \tag{53}$$

is equal to one. In fig. 3 we display the quantities (52) and (53) plotted against each other. That figure shows that, for most points, our model is more similar to the type-I 2HDM, at least in what concerns giving mass to the third generation, *i.e.* the top-quark and bottom-quark masses originate mostly in the Yukawa couplings to *the same* scalar doublet. However, there are also many allowed points for which the quantity (52) is *not* unity; for those points another regularity applies, namely the quantity (53) is very close to zero.
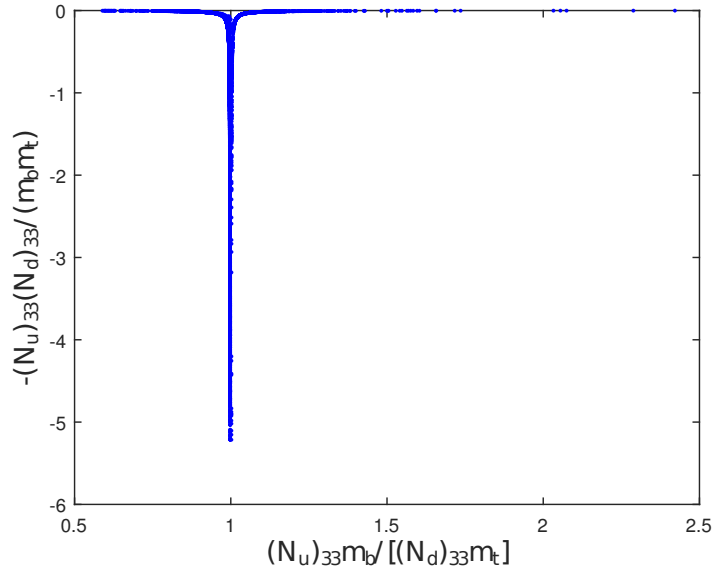
16

Figure 3: $-\left(N_u\right)_{33}\left(N_d\right)_{33}/\left(m_b m_t\right)$ *versus* $\left(N_u\right)_{33} m_b/\left[\left(N_d\right)_{33} m_t\right]$.

Still, one should remember that in our model there is flavour violation in the Yukawa interactions, and one obtains different results from those in figs. 2 and 3 for both the $(1,1)$ and $(2,2)$ entries of both N_d and N_u. In fact, the deviations from either type I- or type II-like behaviour for the first and second generations are much more pronounced than what one observes in fig. 2. But, the corresponding Yukawa couplings being much smaller, that has much less importance for the Higgs-boson phenomenology than the third-generation couplings that we have discussed in those figures.

4.3   Properties of the extra scalars

We now turn to the extra neutral scalars in the model, H and A. The LHC Collaborations have been looking for neutral scalars other than the $125\,\mathrm{GeV}$ boson by investigating the production of W^+W^-, Z^0Z^0, and $\tau\bar{\tau}$, among other channels. The non-observation thus far of meaningful excesses in the cross sections, relatively to their SM expectations, imposes bounds on the masses and couplings of new particles. In our model, the imposition of the top- and meson-physics constraints should force the off-diagonal entries of the matrices N_d and N_u to be smallish, hence we expect that, just as h, the scalars H and A will have reduced flavour-changing interactions. Therefore, our model is expected to behave very much like the flavour-preserving 2HDMs in what concerns the possibility of evading the current experimental non-observation bounds for the extra scalars. As we will now show, there is a vast parameter space still allowed by the experimental constraints.

We firstly consider the limits coming from the search for resonant Z^0Z^0 pairs by both the ATLAS [19, 20, 21, 22, 23] and CMS [24, 25, 26] Collaborations. This is a good channel to look for the heavy CP-even scalar H, which may decay at tree level as $H \to Z^0Z^0$.[11] In fig. 4 we show the points which obey all the constraints described in section 4.1; the points

---

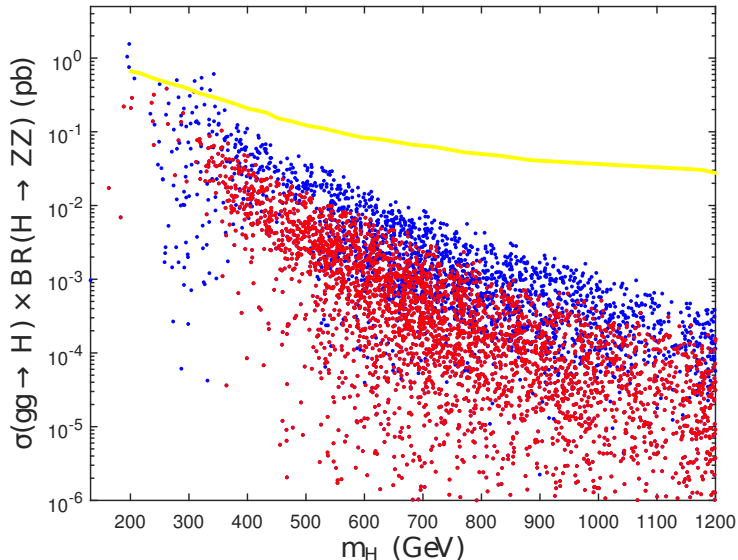[11]Unlike the pseudoscalar A, which may decay to Z^0Z^0 only through loops.

Figure 4: Cross section of the process $pp \to gg \to H \to Z^0 Z^0$ at 13 TeV collision energy, as a function of the mass of the heavy CP-even scalar H. All the points displayed obey the constraints for our model described in subsection 4.1. For the blue points, the 125 GeV scalar h has all its production rates within 20% of their SM-expected values; for the red points those production rates are all within 10% of their SM values. The yellow line is the 2σ upper bound given in ref. [23].

in blue correspond to the requirement that all the μ_X are within 20% of 1, and the points in red have all the μ_X less than 10% away from 1. The yellow line is the upper 2σ bound from the observed limit from ref. [23]. We observe that most of the allowed parameter space yields a $pp \to gg \to H \to Z^0 Z^0$ cross section below the experimental upper bound; only a few low-m_H points exceed the bound, but even for those low values of m_H there are plenty of points which are still allowed. The tighter constraint of 10% on the h production rates does not qualitatively change the picture. There is a simple explanation for why low values of the $pp \to gg \to H \to Z^0 Z^0$ event rate should be obtained, namely, in any CP-conserving 2HDM (or, indeed, multi-Higgs-doublet model) there is the sum rule

$$\left(g_{hZZ}^{\text{2HDM}}\right)^2 + \left(g_{HZZ}^{\text{2HDM}}\right)^2 = \left(g_{hZZ}^{\text{SM}}\right)^2 \qquad (54)$$

for the couplings of the CP-even neutral scalars to gauge-boson pairs. Therefore, if the coupling of h to Z^0 (and $W^\pm$) pairs is very close to its SM value, then the coupling of H to such pairs will be suppressed. Equation (54) is normally expressed through $g_{hZZ}^{\text{2HDM}} = s_{\beta-\alpha}\, g_{hZZ}^{\text{SM}}$ and $g_{HZZ}^{\text{2HDM}} = c_{\beta-\alpha}\, g_{hZZ}^{\text{SM}}$; SM-like behaviour of h means $s_{\beta-\alpha} \simeq 1$, which implies $c_{\beta-\alpha} \simeq 0$.

In fig. 5 (a) we show the gluon–gluon production cross section for a pseudoscalar A, multiplied by its branching ratio to a $t\bar{t}$ pair, at LHC. (Similar results were obtained for H instead of A, but the obtained values of $\sigma \times$ BR were about one order of magnitude lower than those of A.) There are some LHC results for searches in the $t\bar{t}$ channel [27, 28]; we have used the results of ref. [28], although the analysis in that paper does not deal with the
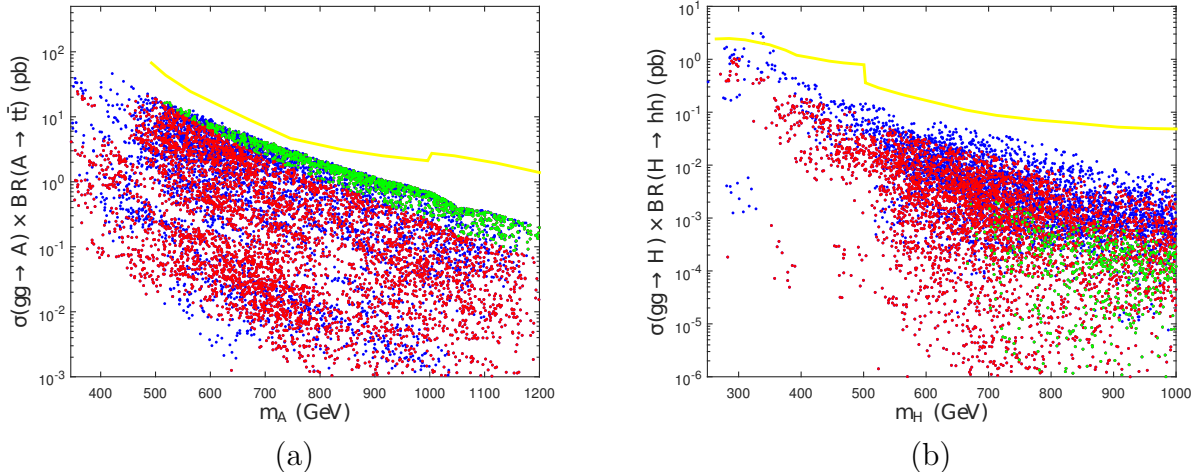
18

Figure 5: (a) The gluon–gluon production and decay to $t\bar{t}$ of the pseudoscalar A *versus* its mass. The yellow line is the upper 2σ bound in figure 11 of ref. [28]. (b) The gluon–gluon production and decay to hh of the scalar H *versus* its mass. All the points displayed obey the constraints described in subsection 4. For the blue points, h has production rates within 20% of its SM-expected values; for the red points those production rates are within 10% of the SM value. The green points are a subset of the red ones, for which the width of the scalar in each plot is larger than 10% its mass. The yellow line is the 2σ upper bound in figure 6 of ref. [29].

2HDM. In fig. 5 (a), the yellow line is the upper 2σ bound in figure 11 of ref. [28].[12] The published results only extend down to $m_A \simeq 500\,\text{GeV}$, but it is clear that no exclusion will occur even for A masses lower than that. As before, the red (blue) points indicate a cut of 10% (20%) on the μ_X ratios for the Higgs boson h, meant to ensure its SM-like behaviour and compliance with the LHC results. The green points in the same plot are the subset of the red ones for which the width of A is larger than 10% of its mass: $\Gamma_A/m_A > 0.1$. We have thus far been assuming the validity of the narrow-width approximation and neglecting eventual interferences between backgrounds and signal; by marking these large-width points in green, we want to draw attention to the only regions where that approximation might fail.[13] The conclusion to draw from fig. 5 (a) is that the current exclusion bounds from the $t\bar{t}$ resonance searches are easily evaded by our model.

In fig. 5 (b) we investigate the possibility of the heavy CP-even scalar H being observed through its decay to two 125 GeV scalars h. This hh channel is being thoroughly studied at the LHC, considering several possible decay channels for both h particles [29, 30, 31, 32, 33, 34, 35, 36, 37]; the yellow line in fig. 5 (b) is the 2σ upper bound of figure 6 of ref. [29]. The blue and red points are the same as before; the green points are the subset of the red ones for which $\Gamma_H/m_H \geq 0.1$. (Therefore, the green points in fig. 5 (b) do *not* coincide with the

---

[12]That figure concerns the possibility of a spin-2 Kaluza–Klein gravitation excitation, and it is the one for which the lowest values of $\sigma \times \text{BR}$ are achieved, as well as the production channel where the initial state includes two gluons; we have chosen it as a conservative option.

[13]Notice, though, that the width of A is never larger than 29.2% of its mass for the points obtained in our fit.
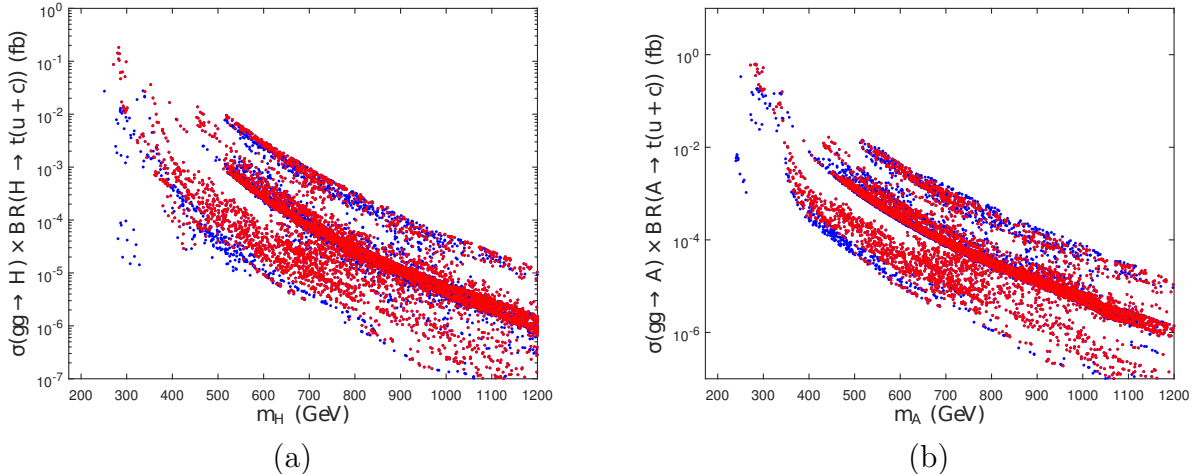
Figure 6: (a) The gluon–gluon production and the decay to tq of (a) the pseudoscalar A and (b) the heavy CP-even scalar H *versus* their respective masses. The colour code is the same as in the previous figures.

green points in fig. 5 (a).) Unlike in fig. 5 (a), the green points, corresponding to scalars H with a large width,[14] correspond to smaller values of $\sigma \times$ BR. Just as in the previous figures, we see that virtually all of our parameter space, except a few low-mass points, complies with the existing experimental bounds.

Since the model that we are studying differs from usual versions of the 2HDM through the existence of FCNC, we have considered the possibility of single-top decays of the heavy (pseudo)scalars H and A. Indeed, the non-diagonal Yukawa interactions lead to the possibility of decays like $H \to t\bar{u}$ and $A \to c\bar{t}$, which might be observed as top-quark + jet events at the LHC; such events should be quite challenging to study in an hadronic machine such as the LHC, but the recent progress in charmed-jet identification algorithms may be a significant contribution for a future analysis.[15] In fig. 6 we present the expected cross section times branching ratio for both (a) the H and (b) the A. In fig. 6 we have grouped together all the FCNC decays of the scalars with a single top in the final state, *viz.* the decays to $t\bar{u}$, $\bar{t}u$, $t\bar{c}$, and $\bar{t}c$. The top- and meson-physics constraints described in subsection 4.1 usually produce N_u matrices with smallish off-diagonal elements, and this yields very small branching ratios for FCNC decays of both H and A—the maximum values that we have obtained were smaller than 5×10^{-4}, but usual values were much smaller than that. Therefore, the model predicts values for $\sigma \times$ BR usually orders of magnitude below the fentobarn. It is difficult to find experimental bounds on such a search channel, but the search for a W' decaying to a single top quark plus a bottom quark [38] can at least give a rough idea of the current sensitivity of the LHC for a top + jet resonance analysis. Though the mass range is different (the analysis of ref. [38] starts at $1\,\text{TeV}$), the bounds shown in that paper for the cross section times the branching ratio are of order $0.1\,\text{pb}$, and therefore much above the predicted $\sigma \times$ BR shown for our model in fig. 6.

---

[14]But, for all the points analyzed the width of H was never larger than 35% of its mass.

[15]We thank Nikolaos Rompotis for this comment.

5 Conclusions

In this paper we have presented a two-Higgs-doublet model that attempts a partial solution of the strong CP problem by relegating a possible generation of a nonzero θ to the two-loop level. Our model achieves this by postulating a soft CP violation that transfers itself just to the CKM matrix, with no CP violation anywhere else in the model, especially no CP violation in scalar–pseudoscalar mixing.

We do not claim that our model achieves a full solution of the strong CP problem, because the θ generated at two-loop level might still be too large. However, since in our model CP violation exists only in the CKM matrix, one may expect θ to be proportional to $J \sim 10^{-5}$, the only CP-violating invariant quantity in that matrix. Adding in a two-loop factor $(16\pi^2)^{-2} \sim 10^{-4}$ and [39] probable suppression factors m_q/m_W, where m_q is a generic second-generation quark mass, one might well reach a sufficiently small θ.

Of course, a 2HDM where CP violation only occurs in the CKM matrix eschews one of the motivations for multi-Higgs-doublet models, namely, obtaining extra sources of CP violation in order to reach a sufficiently large baryon number of the Universe. We have nothing to say about this insufficiency.

We have investigated the compatibility of our model with the outstanding experimental constraints, in particular on the flavour-changing neutral currents. Our model can easily evade them, at the price of cancelations that might be qualified as fine-tuning. We find that the new scalars in our model may in some cases be little heavier than the observed Higgs particle of mass $125\,\text{GeV}$. That will not necessarily make them easy to discover, though, as we have seen in section 4.

A The decay $\bar{B} \to X_s\gamma$

The decays of a bottom-flavoured meson to a strange-flavoured meson and a photon proceed via the quark transition $b \to s\gamma$. Those decays constitute one of the most relevant constraints on the parameter space of a multi-Higgs-doublet model, because they receive important contributions from loops with charged scalars. This is because the interactions of a charged scalar with down-type quarks may be substantially enhanced by ratios of VEVs. Consequently, in a 2HDM the constraints from $b \to s\gamma$ typically eliminate substantial regions of the m_{H^+}–$\tan\beta$ plane.

In the model under discussion in this paper, the occurrence of tree-level FCNC means

that the neutral scalars also contribute to $b \to s\gamma$, unlike what happens in flavour-conserving 2HDMs. We follow the general analysis of ref. [40] to take into account both the charged and the neutral scalars' contributions. We write the Yukawa interactions of our model in the notation

$$\mathcal{L}_{\text{physical}} = \cdots + \sum_{S=h,H,A} S \sum_{k,j=d,s,b} \bar{k} \left(L_{kj}^S P_L + R_{kj}^S P_R \right) j \tag{55a}$$

$$+ \left[H^+ \sum_{\alpha=u,c,t} \bar{\alpha} \sum_{j=b,s,d} \left(L_{\alpha j}^C P_L + R_{\alpha j}^C P_R \right) j + \text{H.c.} \right], \tag{55b}$$

with coefficients defined as[16]

$$L_{kj}^h = \frac{s_{\beta-\alpha} m_k \delta_{kj} - c_{\beta-\alpha} (N_d^*)_{jk}}{v}, \tag{56a}$$

$$R_{kj}^h = \frac{s_{\beta-\alpha} m_k \delta_{kj} - c_{\beta-\alpha} (N_d)_{kj}}{v}, \tag{56b}$$

$$L_{kj}^H = \frac{c_{\beta-\alpha} m_k \delta_{kj} + s_{\beta-\alpha} (N_d^*)_{jk}}{v}, \tag{56c}$$

$$R_{kj}^H = \frac{c_{\beta-\alpha} m_k \delta_{kj} + s_{\beta-\alpha} (N_d)_{kj}}{v}, \tag{56d}$$

$$L_{kj}^A = \frac{i (N_d^*)_{jk}}{v}, \tag{56e}$$

$$R_{kj}^A = \frac{-i (N_d)_{kj}}{v}, \tag{56f}$$

$$L_{\alpha j}^C = \frac{\sqrt{2}}{v} \sum_{\beta=u,c,t} (N_u^*)_{\beta\alpha} V_{\beta j}, \tag{56g}$$

$$R_{\alpha j}^C = -\frac{\sqrt{2}}{v} \sum_{l=d,s,b} V_{\alpha l} (N_d)_{lj}. \tag{56h}$$

The Wilson coefficients required for the computation of $b \to s\gamma$ are [40]

$$C_7'(\mu) = g - \frac{e}{3}, \tag{57a}$$

$$\Delta C_7(\mu) = g' - \frac{e'}{3}, \tag{57b}$$

$$C_8'(\mu) = f + e, \tag{57c}$$

$$\Delta C_8(\mu) = f' + e', \tag{57d}$$

where

$$f = -\frac{v^2}{4V_{ts}^* V_{tb} m_{H^+}^2} \sum_{\alpha=u,c,t} R_{\alpha s}^{C*} \left[R_{\alpha b}^C I_3 \left(\frac{m_\alpha^2}{m_{H^+}^2} \right) + L_{\alpha b}^C \frac{m_\alpha}{m_b} I_4 \left(\frac{m_\alpha^2}{m_{H^+}^2} \right) \right], \tag{58a}$$

---

[16]In our model the matrices N_u and N_d are real, still we write the coefficients in the general form that follows from equation (15), *viz.* allowing for complex N_u and N_d.

$$g = -\frac{v^2}{4V_{ts}^* V_{tb} m_{H^+}^2} \sum_{\alpha=u,c,t} R_{\alpha s}^{C\,*} \left[R_{\alpha b}^C I_5\left(\frac{m_\alpha^2}{m_{H^+}^2}\right) + L_{\alpha b}^C \frac{m_\alpha}{m_b} I_6\left(\frac{m_\alpha^2}{m_{H^+}^2}\right)\right], \qquad (58b)$$

$$e = -\frac{v^2}{4V_{ts}^* V_{tb}} \sum_{S=h,H,A} \frac{1}{m_S^2} \sum_{k=d,s,b} R_{ks}^{S\,*} \left[R_{kb}^S I_3\left(\frac{m_k^2}{m_S^2}\right) + L_{kb}^S \frac{m_k}{m_b} I_4\left(\frac{m_k^2}{m_S^2}\right)\right], \quad (58c)$$

and

$$f' = f\left(R^C \leftrightarrow L^C\right), \tag{59a}$$

$$g' = g\left(R^C \leftrightarrow L^C\right), \tag{59b}$$

$$e' = e\left(R^S \leftrightarrow L^S\right) \text{ for } S = h, H, A. \tag{59c}$$

The functions $I_{3,4,5,6}$ are given in equations (40)–(43) of ref. [40].

To compute the overall branching ratio of $b \to s\gamma$ we follow refs. [41, 42]. We use the effective operators described above, defined as being at the Fermi scale $\mu = m_W$, and include NLO QCD corrections by choosing m_b as the renormalization scale. Let $\eta = \alpha_S\left(m_W\right)/\alpha_S\left(m_b\right) = 0.5651$ [41] be the ratio of the running strong coupling constant between scales m_W and m_b. We compute

$$\Delta C\left(m_b\right) = \eta^{16/23}\,\Delta C_7\left(m_W\right) + \frac{8}{3}\left(\eta^{14/23} - \eta^{16/23}\right)\Delta C_8\left(m_W\right), \tag{60a}$$

$$C'\left(m_b\right) = \eta^{16/23}\,C_7'\left(m_W\right) + \frac{8}{3}\left(\eta^{14/23} - \eta^{16/23}\right)C_8'\left(m_W\right), \tag{60b}$$

and then [43]

$$\mathrm{BR}\left(b \to s\gamma\right) = \mathrm{BR}\left(b \to s\gamma\right)_{\mathrm{SM}} \tag{61a}$$
$$+ \left(2.47 \times 10^{-3}\right)\left\{|\Delta C\left(m_b\right)|^2 + |C'\left(m_b\right)|^2 - 0.706\,\mathrm{Re}[\Delta C\left(m_b\right)]\right\}, \tag{61b}$$

where $\mathrm{BR}\left(b \to s\gamma\right)_{\mathrm{SM}} = 3.15 \times 10^{-4}$. We consider our model to be in compliance with the $b \to s\gamma$ data if it yields a branching ratio within twice the experimental error bar, *viz.* we require $2.4406 \times 10^{-4} < \mathrm{BR}\left(b \to s\gamma\right) < 3.8594 \times 10^{-4}$.

B   The neutral meson–antimeson observables

The FCNC induced by the off-diagonal entries of N_d and N_u lead to tree-level contributions to flavour observables such as CP violation through the parameter ϵ_K and the mass differences in the K^0, B_d^0, B_s^0, and D^0 meson–antimeson systems. These are sensitive observables and new-physics contributions to them may easily be overwhelming. Thus, we must make sure that the contributions to them from the scalar sector of our model conform to the current data. We use the numbers listed in ref. [11].

B.1 K^0–$\bar{K}^0$ observables

Two K^0 meson observables are sensitive to the tree-level FCNC contributions from the scalar sector: the CP-violating parameter ϵ_K and the mass difference between K_S and K_L. Both

observables arise from the matrix element effecting the trasition $\bar{K}^0 \to K^0$, called M_{21}. This receives contributions from the SM, via box diagrams, and from new physics (NP), through FCNC in the scalar sector: $M_{21} = M_{21}^{\mathrm{SM}} + M_{21}^{\mathrm{NP}}$. We use the results presented in ref. [44]. The SM contribution originates in a box diagram and is given by

$$M_{21}^{\mathrm{SM}} = -\frac{G_F^2 m_W^2 f_K^2 m_K B_K}{12\pi^2} \left[\eta_1 \lambda_c^2 S_0(x_c) + \eta_2 \lambda_t^2 S_0(x_t) + 2\eta_3 \lambda_c \lambda_t S_0(x_c, x_t) \right], \qquad (62)$$

where G_F is the Fermi constant, m_W is the W-boson mass, $f_K = 0.1555\,\mathrm{GeV}$ is the K-meson decay constant, $m_K = 0.497611\,\mathrm{GeV}$ is the K-meson mass, and $B_K = 0.723$ parameterizes the error in the vacuum-insertion approximation for the relevant matrix element. The $x_q = (m_q/m_W)^2$ and $\lambda_q = V_{qd}^* V_{qs}$ for $q = c, t$. The functions S_0 are given in equations (B.15) and (B.16) of ref. [44]. Finally, the parameters $\eta_1 = 1.38$, $\eta_2 = 0.57$, and $\eta_3 = 0.47$ account for QCD corrections.

The new-physics contribution originates in the tree-level exchange of h, H, and A. One has, by using the vacuum-insertion approximation for the matrix elements of the operators,[17]

$$M_{21}^{\mathrm{NP}} = \frac{f_K^2 m_K}{96 v^2} \left\{ \left[(N_d^*)_{ds}^2 + (N_d)_{sd}^2 \right] \frac{10 m_K^2}{(m_s + m_d)^2} \left(\frac{1}{m_A^2} - \frac{c_{\beta-\alpha}^2}{m_h^2} - \frac{s_{\beta-\alpha}^2}{m_H^2} \right) \right. \qquad (63a)$$

$$\left. + 4 (N_d^*)_{ds} (N_d)_{sd} \left[1 + \frac{6 m_K^2}{(m_s + m_d)^2} \right] \left(\frac{1}{m_A^2} + \frac{c_{\beta-\alpha}^2}{m_h^2} + \frac{s_{\beta-\alpha}^2}{m_H^2} \right) \right\}. \qquad (63b)$$

Notice that M_{21}^{NP} in our model is *real*.

The K_S–K_L mass difference is given by $\Delta m_K = 2|M_{21}|$. Unfortunately, the SM contribution to Δm_K is affected by considerable uncertainties, stemming from long-distance, difficult to compute contributions to M_{21}^{SM}, and also from imprecisions in the value of B_K. Therefore, we just require that the new-physics term does not give a contribution to Δm_K larger than the experimental value, *i.e.* while fitting the parameters of the model we demand that $2\left| M_{21}^{\mathrm{NP}} \right| < 3.484 \times 10^{-15}\,\mathrm{GeV}$.

It is expected that the uncertainties which trouble the calculation of Δm_K do not affect the computation of ϵ_K, given by

$$\epsilon_K = 2.228 \times 10^{-3} = -\frac{\mathrm{Im}\left(M_{21} \lambda_u^{*2} \right)}{\sqrt{2}\,\Delta m_K\, |\lambda_u|^2}. \qquad (64)$$

In equation (64), we use in the numerator $M_{21} = M_{21}^{\mathrm{SM}} + M_{21}^{\mathrm{NP}}$, while for Δm_K in the denominator we use the experimental value. We accept fit results which give ϵ_K within a 10% deviation from the central value.

B.2 B_H–B_L mass differences

The mass differences in the meson–antimeson B_d^0–$\bar{B}_d^0$ and B_s^0–$\bar{B}_s^0$ systems are well measured and their theoretical calculation, unlike that of Δm_K, is reliable. We use, for the $\bar{B}_d^0 \to B_d^0$ transition,

$$M_{21}^{\mathrm{SM}} = -\frac{G_F^2 m_W^2 f_{B_d}^2 m_{B_d} B_{B_d}}{12\pi^2} \eta_{B_d} \left(V_{tb} V_{td}^* \right)^2 S_0(x_t), \qquad (65)$$

---

[17]See refs. [44] and [7] for a detailed derivation of equation (63).

with $f_{B_d} = 0.1902\,\text{GeV}$, $m_{B_d} = 5.280\,\text{GeV}$, $B_{B_d} = 1.219$, and $\eta_{B_d} = 0.55$. Note that in equation (65) one uses only the box diagram with top-quark internal lines. The NP contribution is given by an expression analogous to equation (63), with the obvious substitutions $f_K \to f_{B_d}$, $m_K \to m_{B_d}$, and $m_s \to m_b$. We accept the result of the fit if $2\left|M_{21}^{\text{SM}} + M_{21}^{\text{NP}}\right|$ is within 10% of the experimental value $\Delta m_{B_d} = 3.333 \times 10^{-13}\,\text{GeV}$.

For the $\bar{B}_s^0 \to B_s^0$ transition we have equation (65) with all indices $d \to s$ and $f_{B_s} = 0.228\,\text{GeV}$, $m_{B_s} = 5.367\,\text{GeV}$, $B_{B_s} = 1.28$, and $\eta_{B_s} = 0.55$. The NP contribution is given by an expression analogous to eq. (63), with the obvious substitutions $f_K \to f_{B_s}$, $m_K \to m_{B_s}$, and $m_d \to m_b$. We accept the result of the fit if $2\left|M_{21}^{\text{SM}} + M_{21}^{\text{NP}}\right|$ is within 10% of the experimental value $\Delta m_{B_s} = 1.17 \times 10^{-11}\,\text{GeV}$.

B.3 The mass difference in the D^0–$\bar{D}^0$ system

There are also contributions to the mass difference in the meson system D^0–$\bar{D}^0$. As in the K^0–$\bar{K}^0$ system, there are considerable uncertainties in the calculation of M_{21}^{SM}. Therefore, once again, we resort to requiring only the New Physics contribution not to be too large. We have

$$M_{21}^{\text{NP}} = \frac{f_D^2 m_D}{96 v^2} \left\{ \left[(N_u^*)_{uc}^2 + (N_u)_{cu}^2\right] \frac{10 m_D^2}{(m_c + m_u)^2} \left(\frac{1}{m_A^2} - \frac{c_{\beta-\alpha}^2}{m_h^2} - \frac{s_{\beta-\alpha}^2}{m_H^2} \right) \right. \tag{66a}$$

$$\left. + 4\,(N_u^*)_{cu}\,(N_u)_{uc} \left[1 + \frac{6 m_D^2}{(m_c + m_u)^2}\right] \left(\frac{1}{m_A^2} + \frac{c_{\beta-\alpha}^2}{m_h^2} + \frac{s_{\beta-\alpha}^2}{m_H^2} \right) \right\}, \tag{66b}$$

with $f_D = 0.212\,\text{GeV}$ and $m_D = 1.865\,\text{GeV}$. Conservatively, we require $2\left|M_{21}^{\text{NP}}\right|$ to be smaller than the measured mass difference $6.253 \times 10^{-15}\,\text{GeV}$.

C $Z \to b\bar{b}$ constraints

A potentially very important constraint to two-Higgs-doublet models (2HDMs) stems from the measurement of the decay $Z \to b\bar{b}$. We follow the treatment of that decay in refs. [45, 46, 47]. The Lagrangian for the $Zb\bar{b}$ vertex is written as

$$\mathcal{L}_{Zb\bar{b}} = -\frac{e Z_\mu}{s_W c_W}\, \bar{b}\,\gamma^\mu \left(\bar{g}_b^L P_L + \bar{g}_b^R P_R \right) b, \tag{67}$$

where the coefficients $\bar{g}_b^{L,R}$ are, at tree level in the SM, $\bar{g}_b^L = -1/2 + s_W^2/3$ and $\bar{g}_b^R = s_W^2/3$. In both the SM and in extensions thereof, these coefficients get one-loop contributions. To wit, in the 2HDM the contributions of loops with charged scalars to $\bar{g}_b^L$ and $\bar{g}_b^R$ are given by

$$\delta \bar{g}_b^L = \frac{\sqrt{2} G_F}{16 \pi^2} \left|(N_u^\dagger V)_{33}\right|^2 f_1\left(\frac{m_t^2}{m_{H^+}^2} \right), \tag{68a}$$

$$\delta \bar{g}_b^R = -\frac{\sqrt{2} G_F}{16 \pi^2} \left|(V N_d)_{33}\right|^2 f_1\left(\frac{m_t^2}{m_{H^+}^2} \right), \tag{68b}$$

where

$$f_1(x) = \frac{x}{x-1} \left(1 - \frac{\ln x}{x-1} \right). \tag{69}$$

The contributions of loops with neutral scalars are expected to be small, both for 2HDMs with flavour conservation [45, 46, 47] or without it [48]; we neglect them. In order to take into account the current experimental results on the observable quantities R_b and A_b (see refs. [45, 11]), we have required that the charged-scalar contribution added to the SM one, viz. $\bar{g}_b^L = -0.42112 + \delta\bar{g}_b^L$ and $\bar{g}_b^R = 0.07744 + \delta\bar{g}_b^R$, does not deviate from the SM prediction by more than 2σ, viz. $2\left(\bar{g}_b^L\right)^2 + 2\left(\bar{g}_b^R\right)^2 = 0.36782 \pm 0.00143$.

D A benchmark point

To illustrate the model, we provide a specific point, which is meant to serve only as an example. The input in the scalar sector is

$$v = \sqrt{v_1^2 + v_2^2} = 246\,\text{GeV}, \quad v_1 = 145.48\,\text{GeV}, \quad \beta - \alpha = 289.46°, \tag{70a}$$

$$m_h = 125\,\text{GeV}, \quad m_H = 688.46\,\text{GeV}, \quad m_A = 364.01\,\text{GeV}, \quad m_{H^+} = 712.00\,\text{GeV}. \tag{70b}$$

To this input correspond the following (approximate) values for the parameters of the scalar potential:

$$\mu_1 = 89682.55\,\text{GeV}^2, \quad \mu_2 = 31942.59\,\text{GeV}^2, \quad \mu_3 = 63188.85\,\text{GeV}^2, \tag{71a}$$

$$\lambda_1 = 9.9708, \quad \lambda_2 = 3.7121, \quad \lambda_3 = 6.8336, \quad \lambda_4 = -12.3750. \tag{71b}$$

It is easy to confirm that the values (71) fulfil all the conditions (23, 24, 25). Notice in equation (70b) that the masses of all four scalars are neither too close nor too far away from each other.

The Yukawa-coupling matrices are as in equations (26), with

$$b_1 = 1.0761 \times 10^{-3}, \quad d_1 = 1.9555 \times 10^{-4}, \quad f_1 = 5.1710 \times 10^{-5}, \tag{72a}$$

$$b_2 = -9.3709 \times 10^{-4}, \quad d_2 = -3.0026 \times 10^{-2}, \quad f_2 = 0, \tag{72b}$$

$$p_1 = 6.9338 \times 10^{-2}, \quad q_1 = -3.0282 \times 10^{-4}, \quad r_1 = -1.3664 \times 10^{-2}, \tag{72c}$$

$$p_2 = -1.2295, \quad q_2 = 0, \quad r_2 = -9.2531 \times 10^{-3}. \tag{72d}$$

We also input $\aleph_1 = 0$, $\aleph_2 = 1.33\,\text{rad}$. One thus obtains quark masses and a CKM matrix in agreement with equations (44, 45). The matrices that parameterize the FCNC are

$$N_d = \begin{pmatrix} 7.4 \times 10^{-3} & 2.7 \times 10^{-2} & 4.2 \times 10^{-2} \\ -1.8 \times 10^{-5} & 0.15 & -5.0 \times 10^{-3} \\ 5.3 \times 10^{-5} & -3.9 \times 10^{-7} & -3.09 \end{pmatrix}, \tag{73a}$$

$$N_u = \begin{pmatrix} 1.2 \times 10^{-2} & -0.29 & -1.61 \\ 6.4 \times 10^{-2} & -0.93 & -14.9 \\ -2.7 \times 10^{-3} & 1.3 \times 10^{-4} & -126 \end{pmatrix}. \tag{73b}$$

One sees that some off-diagonal matrix elements of N_d are not very small, and some off-diagonal matrix elements of N_u—which is almost a triangular matrix—are pretty large. There is a cancelation of about one part in 47 between the contributions to the neutral-D-meson mass difference of the neutral scalars h and H on the one hand and of the pseudoscalar

A on the other hand; there are analogous, yet milder, cancelations among the contributions to the other neutral-meson mass differences. In general, we have found that the D-meson mass difference constraint requires quite strongly fine-tuned cancelations when the neutral scalars have low masses, while the constraints from all other neutral-meson systems are much easier to satisfy and mostly require no fine-tuning. Still, notice that this benchmark point has one particle (the pseudoscalar A) with relatively low mass.

With this benchmark point, the coupling modifiers defined in equations (46) and (48) are

$$\kappa_V = 0.9993, \quad \kappa_t = 0.9721, \quad \kappa_b = 0.9720, \quad \kappa_\tau = 1.0502, \tag{74}$$

and some of the phenomenological quantities computed in section 4 are found to be:

$$\mathrm{BR}\left(h \to q\bar{q}'\right) = 6.89 \times 10^{-11}, \tag{75a}$$
$$\sigma\left(gg \to h\right) = 38.98\,\mathrm{pb}, \tag{75b}$$
$$\sigma\left(gg \to H \to Z^0 Z^0\right) = 0.75\,\mathrm{fb}, \tag{75c}$$
$$\sigma\left(gg \to A \to t\bar{q}_u\right) = 0.03\,\mathrm{fb}, \tag{75d}$$

where (1) $q\bar{q}'$ refers to a sum over all possible FCNC decays of h, (2) the cross sections are for a LHC center-of-mass collision of 13 TeV, (3) the FCNC decays of A involve $q_u = u$ and $q_u = c$, and (4) we have grouped together all the FCNC decays of the scalars with a single top in the final state.

References

[1] J. Dragos, T. Luu, A. Shindler, J. de Vries, and A. Yousif, *Confirming the existence of the strong CP problem in lattice QCD with the gradient flow*, `arXiv:1902.03254 [hep-lat]`.

[2] A. Iwazaki, *Nonvanishing pion masses for vanishing bare quark masses*, `arXiv:1901. 03045 [hep-ph]`.

[3] R. D. Peccei and H. R. Quinn, *CP Conservation in the Presence of Pseudoparticles*, Phys. Rev. Lett. **38** (1977) 1440; *Constraints imposed by CP conservation in the presence of pseudoparticles*, Phys. Rev. D **16** (1977) 1791.

[4] W. A. Bardeen, *Instanton-triggered chiral symmetry breaking, the $U(1)$ problem, and a possible solution to the strong CP problem*, `arXiv:1812.06041 [hep-ph]`.

[5] G. C. Branco, P. M. Ferreira, L. Lavoura, M. N. Rebelo, M. Sher, and J. P. Silva, *Theory and phenomenology of two-Higgs-doublet models*, Phys. Rept. **516** (2012) 1 [`arXiv:1106.0034 [hep-ph]`].

[6] G. Segrè and H. A. Weldon, *Natural Suppression of Strong P- and T-Invariance Violations and Calculable Mixing Angles in SU(2)⊗U(1)*, Phys. Rev. Lett. **42** (1979) 1191.

[7] P. M. Ferreira, L. Lavoura, and J. P. Silva, *A soft origin for CKM-type CP violation*, Phys. Lett. B **704** (2011) 179 [`arXiv:1102.0784 [hep-ph]`].

[8] A. Barroso, P. M. Ferreira, I. P. Ivanov, R. Santos, and J. P. Silva, *Evading death by vacuum*, Eur. Phys. J. C **73** (2013) 2537 [`arXiv:1211.6119 [hep-ph]`].

[9] I. P. Ivanov and J. P. Silva, *Tree-level metastability bounds for the most general two Higgs doublet model*, Phys. Rev. D **92** (2015) 055017 [`arXiv:1507.05100 [hep-ph]`].

[10] A. L. Cherchiglia and C. C. Nishi, *Solving the strong CP problem with non-conventional CP*, `arXiv:1901.02024 [hep-ph]`.

[11] M. Tanabashi *et al.* [Particle Data Group], *Review of Particle Physics*, Phys. Rev. D **98** (2018) 030001.

[12] D. Toussaint, *Renormalization effects from superheavy Higgs particles*, Phys. Rev. D **18** (1978) 1626.

[13] S. Kanemura, Y. Okada, H. Taniguchi, and K. Tsumura, *Indirect bounds on heavy scalar masses of the two-Higgs-doublet model in light of recent Higgs boson searches*, Phys. Lett. B **704** (2011) 303 [`arXiv:1108.3297 [hep-ph]`].

[14] P. M. Ferreira, J. F. Gunion, H. E. Haber, and R. Santos, *Probing wrong-sign Yukawa couplings at the LHC and a future linear collider*, Phys. Rev. D **89** (2014) 115003 [`arXiv:1403.4736 [hep-ph]`].

[15] P. M. Ferreira, R. Guedes, M. O. P. Sampaio, and R. Santos, *Wrong sign and symmetric limits and non-decoupling in 2HDMs*, JHEP **1412** (2014) 067 [`arXiv:1409.6723 [hep-ph]`].

[16] R. V. Harlander, S. Liebler, and H. Mantler, *SusHi: A program for the calculation of Higgs production in gluon fusion and bottom-quark annihilation in the Standard Model and the MSSM*, Comput. Phys. Commun. **184** (2013) 1605 [`arXiv:1212.3249 [hep-ph]`].

[17] R. V. Harlander, S. Liebler, and H. Mantler, *SusHi Bento: Beyond NNLO and the heavy-top limit*, Comput. Phys. Commun. **212** (2017) 239 [`arXiv:1605.03190 [hep-ph]`].

[18] M. Nebot and J. P. Silva, *Self-cancellation of a scalar in neutral meson mixing and implications for the LHC*, Phys. Rev. D **92** (2015) 085010 [`arXiv:1507.07941 [hep-ph]`].

[19] M. Aaboud *et al.* [ATLAS Collaboration], *Search for WW/WZ resonance production in ℓνqq final states in pp collisions at $\sqrt{s} = 13\,TeV$ with the ATLAS detector*, JHEP **1803** (2018) 042 [`arXiv:1710.07235 [hep-ex]`].

[20] M. Aaboud *et al.* [ATLAS Collaboration], *Searches for heavy ZZ and ZW resonances in the ℓℓqq and ννqq final states in pp collisions at $\sqrt{s} = 13\,TeV$ with the ATLAS detector*, JHEP **1803** (2018) 009 [`arXiv:1708.09638 [hep-ex]`].

[21] M. Aaboud *et al.* [ATLAS Collaboration], *Search for heavy resonances decaying into WW in the eνμν final state in pp collisions at $\sqrt{s} = 13\,TeV$ with the ATLAS detector*, Eur. Phys. J. C **78** (2018) 24 [`arXiv:1710.01123 [hep-ex]`].

[22] ATLAS Collaboration, *Study of the Higgs boson properties and search for high-mass scalar resonances in the $H \rightarrow ZZ^* \rightarrow 4\ell$ decay channel at $\sqrt{s} = 13\,TeV$ with the ATLAS detector*, ATLAS-CONF-2016-079.

[23] ATLAS Collaboration, *Search for heavy ZZ resonances in the $\ell^+\ell^-\ell^+\ell^-$ and $\ell^+\ell^-\nu\bar{\nu}$ final states using proton–proton collisions at $\sqrt{s} = 13\,TeV$ with the ATLAS detector*, ATLAS-CONF-2017-058.

[24] CMS Collaboration, *Search for a heavy scalar boson decaying into a pair of Z bosons in the $2\ell2\nu$ final state*, CMS-PAS-HIG-16-001.

[25] CMS Collaboration, *Measurements of properties of the Higgs boson and search for an additional resonance in the four-lepton final state at $\sqrt{s} = 13\,TeV$*, CMS-PAS-HIG-16-033.

[26] CMS Collaboration, *Search for new diboson resonances in the dilepton + jets final state at $\sqrt{s} = 13\,TeV$ with 2016 data*, CMS-PAS-HIG-16-034.

[27] M. Aaboud *et al.* [ATLAS Collaboration], *Search for Heavy Higgs Bosons A/H Decaying to a Top Quark Pair in pp Collisions at $\sqrt{s} = 8\,TeV$ with the ATLAS Detector*, Phys. Rev. Lett. **119** (2017) 191803 [arXiv:1707.06025 [hep-ex]].

[28] M. Aaboud *et al.* [ATLAS Collaboration], *Search for heavy particles decaying into a top-quark pair in the fully hadronic final state in pp collisions at $\sqrt{s} = 13\,TeV$ with the ATLAS detector*, arXiv:1902.10077 [hep-ex].

[29] G. Aad *et al.* [ATLAS Collaboration], *Searches for Higgs boson pair production in the $hh \rightarrow bb\tau\tau$, $\gamma\gamma WW^*$, $\gamma\gamma bb$, bbbb channels with the ATLAS detector*, Phys. Rev. D **92** (2015) 092004 [arXiv:1509.04670 [hep-ex]].

[30] ATLAS Collaboration, *Search for Higgs boson pair production in the $b\bar{b}\gamma\gamma$ final state using pp collision data at $\sqrt{s} = 13\,TeV$ with the ATLAS detector*, ATLAS-CONF-2016-004.

[31] CMS Collaboration, *Search for Higgs boson pair production in the final state containing two photons and two bottom quarks in proton–proton collisions at $\sqrt{s} = 13\,TeV$*, CMS-PAS-HIG-17-008.

[32] M. Aaboud *et al.* [ATLAS Collaboration], *Search for pair production of Higgs bosons in the $b\bar{b}b\bar{b}$ final state using proton–proton collisions at $\sqrt{s} = 13\,TeV$ with the ATLAS detector*, Phys. Rev. D **94** (2016) 052002 [arXiv:1606.04782 [hep-ex]].

[33] CMS Collaboration, *Search for heavy resonances decaying to a pair of Higgs bosons in the four b quark final state in proton–proton collisions at $\sqrt{s} = 13\,TeV$*, CMS-PAS-B2G-16-026.

[34] ATLAS Collaboration, *Search for pair production of Higgs bosons in the $b\bar{b}b\bar{b}$ final state using proton–proton collisions at $\sqrt{s} = 13\,TeV$ with the ATLAS detector*, ATLAS-CONF-2016-049.

[35] ATLAS Collaboration, *Search for Higgs boson pair production in the final state of* $\gamma\gamma WW^*(\to l\nu jj)$ *using 13.3 fb^{-1} of pp collision data recorded at* $\sqrt{s} = 13\,TeV$ *with the ATLAS detector*, ATLAS-CONF-2016-071.

[36] A. M. Sirunyan *et al.* [CMS Collaboration], *Search for resonant and nonresonant Higgs boson pair production in the* $b\bar{b}\ell\nu\ell\nu$ *final state in proton–proton collisions at* $\sqrt{s} = 13\,TeV$, JHEP **1801** (2018) 054 [arXiv:1708.04188 [hep-ex]].

[37] A. M. Sirunyan *et al.* [CMS Collaboration], *Search for Higgs boson pair production in events with two bottom quarks and two tau leptons in proton–proton collisions at* $\sqrt{s} = 13\,TeV$, Phys. Lett. B **778** (2018) 101 [arXiv:1707.02909 [hep-ex]].

[38] M. Aaboud *et al.* [ATLAS Collaboration], *Search for* $W' \to tb$ *decays in the hadronic final state using pp collisions at* $\sqrt{s} = 13\,TeV$ *with the ATLAS detector*, Phys. Lett. B **781** (2018) 327 [arXiv:1801.07893 [hep-ex]].

[39] J. R. Ellis and M. K. Gaillard, *Strong and weak CP violation*, Nucl. Phys. B **150** (1979) 141.

[40] L. Lavoura, *General formulae for* $f_1 \to f_2\gamma$, Eur. Phys. J. C **29** (2003) 191 [hep-ph/0302221].

[41] A. J. Buras, M. Misiak, M. Münz, and S. Pokorski, *Theoretical uncertainties and phenomenological aspects of* $B \to X_s\gamma$ *decay*, Nucl. Phys. B **424** (1994) 374 [hep-ph/9311345].

[42] M. Misiak and M. Steinhauser, *NNLO QCD corrections to the* $\bar{B} \to X_s\gamma$ *matrix elements using interpolation in* m_c, Nucl. Phys. B **764** (2007) 62 [hep-ph/0609241].

[43] M. Blanke, B. Shakya, P. Tanedo, and Y. Tsai, *The birds and the Bs in RS: the* $b \to s\gamma$ *penguin in a warped extra dimension*, JHEP **1208** (2012) 038 [arXiv:1203.6650 [hep-ph]].

[44] G. C. Branco, L. Lavoura, and J. P. Silva, *CP Violation* (Oxford University Press, 1999).

[45] H. E. Haber and H. E. Logan, *Radiative corrections to the* $Zb\bar{b}$ *vertex and constraints on extended Higgs sectors*, Phys. Rev. D **62** (2000) 015011 [hep-ph/9909335].

[46] O. Deschamps, S. Monteil, V. Niess, S. Descotes-Genon, S. T'Jampens, and V. Tisserand, *Two Higgs Doublet of type II facing flavor physics data*, Phys. Rev. D **82** (2010) 073012 [arXiv:0907.5135 [hep-ph]].

[47] G. Degrassi and P. Slavich, *QCD corrections in two-Higgs-doublet extensions of the standard model with minimal flavor violation*, Phys. Rev. D **81** (2010) 075001 [arXiv:1002.1071 [hep-ph]].

[48] J. Hernandez-Sánchez, S. Moretti, R. Noriega-Papaqui, and A. Rosado, *Off-diagonal terms in Yukawa textures of the type-III 2-Higgs doublet model and light charged Higgs boson phenomenology*, JHEP **1307** (2013) 044 [arXiv:1212.6818 [hep-ph]].